Development and Characterization of Alumina-CNTs composite Membranes for Water Filtration Application

BY

HAFIZ KHURRAM SHAHZAD

A Thesis Presented to the
DEANSHIP OF GRADUATE STUDIES

KING FAHD UNIVERSITY OF PETROLEUM & MINERALS

DHAHRAN, SAUDI ARABIA

In Partial Fulfillment of the
Requirements for the Degree of

MASTER OF SCIENCE

In

MATERIALS SCIENCE AND ENGINEERING

MAY, 2017

KING FAHD UNIVERSITY OF PETROLEUM & MINERALS

DHAHRAN- 31261, SAUDI ARABIA

DEANSHIP OF GRADUATE STUDIES

This thesis, written by **Hafiz Khurram Shahzad** under the direction his thesis advisor and approved by his thesis committee, has been presented and accepted by the Dean of Graduate Studies, in partial fulfillment of the requirements for the degree of **MASTER OF SCIENCE IN MATERIALS SCIENCE & ENGINEERING.**

Dr. Tahar Laoui
(Advisor)

Dr. Zuhair M. Gasem
Department Chairman

Dr. Zafarullah Khan
(Member)

Dr. Salam A. Zummo
Dean of Graduate Studies

Dr. Abbas S. Hakeem
(Member)

31/5/17

Date

To my family for their love and support

ACKNOWLEDGMENTS

In the name of Allah, the most Gracious and the most Merciful. First, I would like to thank almighty Allah who gave me health, peace of mind and strength to accomplish this milestone. I would like to express my deepest gratitude to my family (my parents and my wife) for their continuous encouragement and unflagging support throughout the period of my MS degree. I want to extend my sincere appreciation for the Department of Mechanical Engineering, King Fahd University of Petroleum and Minerals (KFUPM) for giving me fully funded scholarship during my masters' study. I would also like to acknowledge King Abdulaziz City of Science and Technology (KACST) to provide funding for my thesis research project.

In KFUPM, I'm truly indebted to Dr. Tahar Laoui, my thesis advisor, for his consistent support, guidance, motivation, kind words, help, and encouragement to complete my thesis successfully. I feel lucky of having such a nice person as my supervisor. I am also grateful to Dr. Zafarullah Khan and Dr. Abbas S. Hakeem, my committee members, for their cooperation, suggestions, and support. I'm also thankful to Dr. Abdrabou Hussein and Mr. F. Patel for their support and contribution to my work.

I offer my sincere gratitude to all the staff in the Center of Research Excellence in Nano Technology (CENT, KFUPM), especially Dr. Zain Hassan Yamani, Dr. Abbas Hakeem, and Dr. Nasiruzzaman Sheikh, for giving me the opportunity to learn and get experienced on the state-of-the-art machinery. CENT equipped me with hands-on experience in the latest materials characterization techniques like FESEM, XRD, TGA, TMA, DSC, DMA, SPS, HEBM, and more.

I’m highly obliged to all staff of Materials Science and Chemical Engineering labs who helped me to perform the experimentations; especially Mr. Latif Hashmi, Mr. Tajudeen A. Oyehan, Mr. Amanullah. In addition, I’m also very thankful to all my KFUPM friends especially Raja Awais, Waleed Umar, Moath Al-Malki, M. Umer, Abdul Waheed, Azhar Khan, Umar Hayat, M. Faizan, Hafiz ur Rahman, and Bilal Anjum who supported me in various aspects during my stay in KFUPM.

TABLE OF CONTENTS

ACKNOWLEDGMENTS ..... **V**

TABLE OF CONTENTS ..... **VII**

LIST OF TABLES ..... **X**

LIST OF FIGURES ..... **XI**

LIST OF ABBREVIATIONS ..... **XIII**

ABSTRACT ..... **XIV**

ملخص الرسالة ..... **XVI**

CHAPTER 1 INTRODUCTION **1**

1.1 Overview **1**

1.2 Aim/Objectives **6**

1.3 Organization of the thesis **7**

CHAPTER 2 LITERATURE REVIEW **8**

2.1 Sources of heavy metal ions **8**

2.2 Hazards associated with heavy metals **9**

2.3 Need to remove heavy metals **10**

2.4 Conventional techniques for heavy metal removal **11**

2.5 Adsorption **11**

2.6 Conventional Adsorbents **12**

2.7 Adsorption through alumina **13**

2.8 Adsorption through carbon nanotubes (CNTs) 15

2.9 Separation through CNT-based composite membranes 23

2.10 Powder metallurgical method to develop ceramic membranes 27

2.10.1 Pressure-less solid state sintering 27

2.10.2 Spark plasma sintering 30

CHAPTER 3 MATERIALS AND EXPERIMENTAL PROCEDURE 31

3.1 Materials 31

3.2 Experimental Procedure 33

3.2.1 Powder Preparation 33

3.2.2 Membrane synthesis by conventional pressure-less sintering 35

3.2.3 Membrane synthesis by spark plasma sintering (SPS) 38

3.3 Characterization Techniques 39

3.3.1 X-ray diffraction (XRD) 39

3.3.2 Field Emission Scanning Electron Microscopy (FE-SEM) 39

3.3.3 Water Permeation Test 39

3.3.4 Porosity measurement 40

3.3.5 Diametrical compression test 41

3.4 Heavy metal removal test 42

CHAPTER 4 RESULTS AND DISCUSSION 44

4.1 Pressure-less Solid State Sintering 44

4.1.1 Effect of sintering temperature 47

4.1.2 Effect of initial compaction load 49

4.2 Spark Plasma Sintering (SPS) 53

4.2.1 Characterization of the starting materials 54

4.2.2 Effect of SPS parameters on porosity, water flux, and permeability 56

4.2.3 Microstructure characterization of SPS membrane 58

4.2.4 Mechanical properties of alumina-CNTs membrane 60

4.3 Removal of cadmium heavy metal from aqueous solution 62

CHAPTER 5 CONCLUSIONS AND RECOMMENDATIONS 66

5.1 Conclusions 66

5.2 Recommendations 67

REFERENCES **68**

VITAE **77**

LIST OF TABLES

Table 2-1: Industries producing heavy metals [32] 9
Table 2-2: Health risk associated with heavy metals & MCL standards [34] 10
Table 2-3: Comparison of alumina with other adsorbents [47] 15
Table 2-4: Comparison of adsorption capacity of CNTs & other adsorbents for heavy metals [82] 21
Table 4-1: Experimental Design (Characteristics of various membranes prepared at different process parameters) 45
Table 4-2: SPS processing parameters, porosity, and diametrical strength 54

LIST OF FIGURES

Figure 2-1: Comparative study of different adsorbents towards heavy meat adsorption [52] 14
Figure 2-2: (a) MWCNTs (b) SWCNTs [60] 16
Figure 2-3: Four possible adsorption sites on the nano bundle [63] 17
Figure 2-4: Plasma technique to generate FG on CNT surface [73] 20
Figure 2-5: Chemisorption of metal ions by functional groups present on CNT surface [83] 22
Figure 2-6: Schematic of CNT/PA membrane developed through CVD growth of CNTs inside the alumina pores 24
Figure 2-7: Vertically aligned CNTs on alumina template [87] 25
Figure 2-8: FE-SEM images of porous alumina matrix (a) before CNTs growth (b) after CNTs growth 26
Figure 2-9: Randomly oriented CNTs on mullite substrate [91] 26
Figure 2-10: (a) water flux (b) Ni ion rejection from CNT-mullite membrane 27
Figure 3-1: Raw materials used for powder mixture preparation 32
Figure 3-2: Flow chart representing alumina-CNTs membrane synthesis 34
Figure 3-3: Compaction process of alumina-CNTs powder mixture 36
Figure 3-4: Pressure-less solid state sintering process 37
Figure 3-5: Spark plasma sintering (SPS) facility 38
Figure 3-6: Flow loop system used for water flux measurement and heavy metal removal test 40
Figure 3-7: Schematic of diametrical compression test (b, c) Alumina-CNT membrane before and after the test 41
Figure 3-8: Batch adsorption test 42
Figure 3-9: Inductively-coupled plasma optical emission spectroscopy (ICP-OES) for Cd conc. Test 43
Figure 4-1: (a) XRD pattern (i) CNTs (ii) alumina (iii) powder mixture (alumina-5wt% CNTs) (b): Membranes compacted at (i) 50 kN (ii) 100 kN (iii) 150 kN (iv) 200 kN and sintered at 1400° C 46
Figure 4-2: FE-SEM micrographs of as-received powders (a) α-alumina (b) raw CNTs 46
Figure 4-3: Membranes compacted with 50 kN and sintered at (a) 1200° C (b) 1300° C (c) 1400° C (d) 1500° C 48
Figure 4-4: (a) Porosity and (b) strength relationship of the membranes with the change in sintering temperature (compaction load was 50 kN) 48
Figure 4-5: FE-SEM images of the membranes compacted at (a) 50 kN (b) 100 kN (c) 150 kN (d) 200 kN loads and sintered at 1400° C 49
Figure 4-6: FE-SEM images of the membranes compacted at (a) 50 kN (b) 100 kN (c) 150 kN (d) 200 kN loads and sintered at 1500° C 50

Figure 4-7: (a) Porosity and (b) strength relationship of the membranes with the change in compaction load (sintering temperatures were 1400° C and 1500° C)..... 51
Figure 4-8: Effect of compaction load on water flux sintered at (a) 1400°C (b) 1500°C 52
Figure 4-9: FE-SEM image of the as-received materials: (a) α-alumina (b) CNTs 55
Figure 4-10: XRD patterns of (a) as received CNTs, (b) as received α-alumina, (c) sintered sample at 10 MPa,1100°C,5 min, 200° C/min)..... 55
Figure 4-11: Effect of SPS parameters on the porosity and permeability of the membranes: (a) Pressure, (b) Heating rate, (c) Holding time, and (d) Temperature..... 56
Figure 4-12: Effect of different SPS parameters on pure water flux at different transmittance pressure: (a) Pressure, (b) Heating rate, (c) Holding time, and (d) Temperature 57
Figure 4-13: FE-SEM of the membrane SPS at different pressure: (a)5.6 MPa, 1000°C, 10 min, 100° C/min, and (b) 10 MPa, 1000° C,10 min, 100° C/min 59
Figure 4-14: FE-SEM of the membrane SPS at 10 MPa, 1100° C, 5 min, 200° C/min.... 60
Figure 4-15: FE-SEM micrograph of fracture surfaces of SPS at 10 MPa, 1000° C,10 min, 50° C/min..... 60
Figure 4-16: Diametrical compression test: (a) configuration, (b) sample before the test, (c) Sample after the test..... 61
Figure 4-17: permeability and strength of the membrane at different SPS conditions..... 62
Figure 4-18: Effect of pH on cd^{+2} removal (Batch experimental runs) 63
Figure 4-19: Zeta potential analysis of alumina and CNTs powders as a function of pH 64
Figure 4-20: Comparison of the removal efficiency of alumina, CNTs, alumina-5wt% CNTs powder mixture and fabricated membrane of same composition 65

LIST OF ABBREVIATIONS

α-Al_2O_3	:	Alpha-alumina
CNT	:	Carbon Nanotubes
MWCNT	:	Multi-walled Carbon Nanotubes
AC	:	Activated Carbon
CVD	:	Chemical Vapor Deposition
SPS	:	Spark Plasma Sintering
Cd	:	Cadmium (Heavy metal)
ICP-OCS	:	Inductively Coupled Plasma Optical Emission Spectroscopy
MCL	:	Maximum Concentration Limit
GA	:	Gum Arabic
SDS	:	Sodium Dodecyl Sulfate
PVA	:	Poly Vinyl Alcohol
SEM	:	Scanning Electron Microscopy
XRD	:	X-Ray Diffraction

ABSTRACT

Full Name : [Hafiz Khurram Shahzad]

Thesis Title : [Development and characterization of alumina-CNTs nanocomposite membranes for water filtration application]

Major Field : [Materials Science and Engineering]

Date of Degree : [May 2017]

Porous alumina-carbon nanotubes (Al_2O_3-CNTs) nanocomposite membrane was developed via powder metallurgical techniques (conventional pressure-less and spark plasma sintering). In conventional pressure-less solid state sintering, the membrane was fabricated into circular disk (27 mm diameter and 4 mm thickness) by uniaxial pressing of the composite powder mixture (Al_2O_3-5wt%CNTs) followed by sintering in a tube furnace under inert (Ar) atmosphere. Homogeneous dispersion of CNTs within the alumina matrix was achieved using gum Arabic (GA) and sodium dodecyl sulfate (SDS) as dispersants in the powder mixture. The synthesized membrane was characterized using X-Ray Diffraction (XRD) for phase analysis and Field Emission Scanning Electron Microscopy (FE-SEM) for microstructural analysis. The effect of process parameters (initial powder compaction load and sintering temperature) on the overall performance of the membrane (in terms of porosity, strength, and water flux) was investigated. The results showed that the membrane's properties were strongly influenced by the process parameters. The porosity of the membrane was observed to decrease from 65% to 31% while strength increased from 0.76 MPa to 15.64 MPa when both compaction load and sintering temperature increased from (50 kN to 200 kN) and (1200° C to 1500° C), respectively. Moreover, spark plasma sintering (SPS) technique was utilized to develop the same

membrane in which compaction pressure and sintering were carried out simultaneously. The effect of SPS processing parameters including pressure, temperature, heating rate, and holding time on porosity, water flux, permeability and mechanical properties of the developed membranes was analyzed and correlated with the processing parameters to obtain the best combination of the membrane permeability and strength. The results revealed that CNTs were well distributed in the alumina matrix and located mainly at the alumina grain boundary. The porosity of the developed SPS-membrane varied from 10.8% to 69.7%. The porosity and strength were highly influenced by sintering pressure and temperature. The findings revealed that the membranes sintered at (10 MPa, 1100° C, 200° C/min, 5 min), possessing an average pore size of 143 nm, showed the best combination of permeability (38 L/m^2.hr.bar) and strength (9.5 MPa). Selected membranes developed from conventional (200 kN/1400° C) as well as SPS (10MPa, 1100°C, 200° C/min, 5 min) methods were utilized for cadmium removal, mainly through physical adsorption, using 1 ppm aqueous solution at pH 6 and rejected 93% and 88% of Cd^{+2} ions, respectively, from aqueous solution in a single pass. The developed membranes offer a good potential for water treatment application.

ملخص الرسالة

الاسم الكامل: **حافظ خرم شهزاد**

عنوان الرسالة: تطوير واختبار الأغشية النانوية المركبة من أكسيد الألمنيوم و أنابيب الكربون النانوية لتطبيقات تنقية المياه

التخصص: هند سة وعلوم مواد

تاريخ الدرجة العلمية: **مايو 2017**

يقدم هذا البحث ولأول مرة طريقة تصنيع الأغشية النانوية المركبة من أكسيد الألمنيوم وأنانيب الكربون النانوية باستخدام تقنية البلازما والشرارة الكهربائية و تقنية التصليب التقليدية بدون استخدام الضغط، والتي تم فيها- أي التقنية الأخيرة- تصنيع الأغشية في صورة أقراص دائرية (قطرها 27 مم وسماكتها 4 مم) باستخدام الضغط أحادي المحور لخليط المساحيق ، والذي تبعه تقنية التصليب التقليدية بدون استخدام الضغط. لوحظ توزيع أنابيب الكربون النانوية المتجانس في مصفوفة أكسيد الألمنيوم باستخدام مشتتات اللبان العربي و دوديسيل كبريتات صوديوم. اختبرت الأغشية المصنعة باستخدام تقنية حيود الأشعة السينية لتحليل الأطوار ، وباستخدام المجهر الأليكتروني لتحليل التركيب المجهري.

فحص البحث أثر متغيرات عملية التحضير باستخدام تقنية التصليب التقليدية (وزن الضغط الأولي و درجة حرارة التصليب) على الأداء الكلي للغشاء (من جهة المسامية والقوة و تدفق المياه)، والتي ثبت اعتمادها بشكل كبير على متغيرات عملية التحضير. لوحظ انخفاض مسامية الغشاء من 65% إلى 31% وزيادة القوة من 0.76 MPa إلى 15.64 MPa عندما انخفض وزن الضغط من 50 kN إلى 200 kN وارتفعت درجة الحرارة من 1200 °C إلى 1500 °C . استفاد البحث من تقنية التصليب بالبلازما والشرارة الكهربائية لتحضير ذات الغشاء، حيث تزامنت عملية الضغط مع عملية التصليب في آن واحد. حلل أثر متغيرات عملية التصليب، كالضغط ودرجة الحرارة و معدل التسخين و زمن العملية، على مسامية الغشاء و تدفق المياه و النفاذية و الخصائص الميكانيكية، للحصول على أفضل قيم من نفاذية الفشاء و قوته معا.

أوضحت نتائج الدراسة توزع أنانيب الكربون النانوية المتجانس في مصفوفة أكسيد الألمنيوم، وبشكل أخص في أطراف الحبيبات. أمكن التحكم في مسامية الغشاء عن طريق متغيرات عملية التصليب بالبلازما والشرارة الكهربائية، حيث تراوحت قيمتها- أي المسامية- بين 10.8% و 69.7%، و التي تأثرت – إلى جانب قوة الغشاء- بدرجة حرارة التصليب و الضغط. وجد أن العينات المصلبة على ضغط 10 MPa ودرجة حرارة 1100 ˚C لمدة 5 min باستخدام معدل تسخين 200 ˚C/min تحصلت على حجم فجوة بمعدل 143 نانومتر، مظهرة بذلك أفضل قيم للنفاذية والقوة معا. اختبر

البحث قدرة الأغشية النانوية المركبة من أكسيد الألمنيوم وأنانبيب الكاربون النانوية على تصفية معدن الكادميوم بتجربة الامتزاز بنظام حلقة التدفق. أوضح هذا الاختبار قدرة هذه الأغشية على تصفية 93% من معدن الكادميوم بعملية الامتزازمن عينة ماء تحتوي على 1ppm من الكادميوم برقم هيدروجيني يساوي 6

CHAPTER 1

INTRODUCTION

1.1 Overview

Meeting the human needs of clean and affordable water is a great challenge of 21st century. It is the humanitarian goal worldwide to fulfill the continuously increasing demands for clean water. According to World Health Organization (WHO), still more than 700 million people on the planet do not have access to clean water. [1]

With continuously increasing global population and living standards, it has become difficult to meet the demands of clean drinking water by conventional water supplies. Therefore, it is needed to explore new and non-conventional water resources (such as contaminated water, wastewater, sea water and brackish water) to meet the challenge. [2]

Heavy metals are serious cause of contamination in water that create great hindrance in smooth water recovery. Pollutants, including heavy metals, are discharged into the freshwater lakes and rivers from industries, agricultural and domestic sources. These heavy metals not only deposit into the sediments but engulf various organisms and, thus, aquatic life in the ecosystem comes into direct contact with them. These heavy metals are non-biodegradable in nature and accumulate into aquatic organisms such as fish, oysters, mussels. and enter the food chain. Excessive amounts of the heavy metals are toxic to aquatic organisms as well as human beings. Human exposure to heavy metals is highly toxic and has serious health implications. [3]

Extensive research has been done and various commercial techniques are available to mitigate the heavy metal pollution. The most commonly applied methods are: (i) precipitation as hydroxides, carbonates or sulfides, (ii) sorption (adsorption, ion exchange), (iii) membrane-based processes, (iv) electrolytic recovery, (vi) liquid–liquid extraction and (vii) flotation. [4]–[7] However, adsorption and membrane separation are considered the most effective methods. In adsorption, adsorbates are physically (physisorption) or chemically (chemisorption) attached to the surface of the adsorbent and hence removed from the liquid medium. Different types of natural adsorbents (coconut husk, pine wood, zeolite, char, carbon powders, minerals, oak bark, clay and cellulose), synthetic adsorbents (fly ash, various metallic oxides, activated carbon, activated alumina, CNTs slags and polymers) have been studied extensively to mitigate the metallic pollution. [2], [7]–[10]

From the last few decades, inorganic membranes have gained more attention in water treatment and other industrial applications i.e. food, pigment, chemical, environmental, and pharmaceutical. The importance of these membranes is attributed to their superior characteristics like chemical inertness, thermal stability, corrosion resistance, and high separation efficiency. [11]–[19] Conventional ceramic processing methods (dry pressing, paste pressing or colloidal pressing) followed by sintering have commonly been used to fabricate porous ceramic supports having the adequate mechanical strength for ceramic membranes. [20] The selection of suitable raw materials, processing method, and sintering technique has great influence on the final porous structured membrane. [21] Ceramic porous bodies are commonly synthesized by compacting the starting powder into desired shape followed by sintering. The properties of a consolidated porous ceramic body (e.g. pore size, porosity and strength) depend on the processing parameters such as sintering

temperature, time, and heating rate. [22] Barma and Mandal investigated the initial compaction load and sintering temperature on the porosity, mechanical strength and pore size of the membrane. The lower the sintering temperature or the initial compaction load is higher the final porosity with a larger average pore size of the membrane is. However, strength increases by increasing compaction load or sintering temperature due to higher grain densification and lower porosity. [23] S. Hashimoto et al, synthesized a porous alumina body using alumina platelets by varying compaction pressure (1 to 3 MPa) at constant sintering temperature (1400 °C) and measured densities of 25% and 35.5%, respectively. [24] The mechanical properties of porous alumina structures have a correlation with the total porosity and relative density. F. Patel et al, also studied the effect of compaction pressure (230-620 MPa followed by sintering at 1400 °C) on the final density of porous alumina substrates made from alumina particles (average particle size of 0.3 μm). They observed an increase in mechanical strength with increasing initial compaction pressure. [25]

Porous ceramic membranes have been manufactured using a variety of materials such as clay [26], zirconia [27], titania [28], silica [29] and fly ash [30]. However, alumina is one of the most commonly used materials to fabricate porous membrane supports for asymmetric membranes [26]-[31] as well as ceramic membrane filter. [32][33][34] Alumina has also been utilized because of its excellent adsorption properties for metal ions. [35]–[37] Yabe and Oliveira investigated the adsorption adsorbate ratio and the contact time of metal ions on alumina from the industrial effluent. They reported that alumina (Al_2O_3) exhibited excellent adsorption efficiency for the removal of Fe, Cr, Pb, Ni, Cd, Cu and Zn. [38]

Recent advances in nanotechnology coupled with membrane separation has opened new doors of exploration to enhance the membrane performance with synergistic effect on wastewater treatment. [39] Carbon nanotubes (CNTs) are relatively new adsorbents and have proven to possess great potential for heavy metal removal. CNTs are promising for environmental applications because of their unique properties such as large specific surface area, high porosity, low density, high mechanical strength, high thermal and chemical stability, and strong interaction between pollutant molecules and the CNTs surfaces. [40]–[44] Therefore, it could be worthwhile to combine both adsorbents (alumina and CNTs) to produce a porous nanocomposite membrane. Although, extensive literature is available on alumina-CNTs composite to describe its electrical, mechanical, thermal, tribological properties but most of the literature is on solid dense composites and limited work is reported on porous alumina-CNTs membrane. To produce CNTs-based ceramic membranes, chemical vapor deposition (CVD) method has been used to grow CNTs on the ceramic template. Tariq Altalhi et al, fabricated carbon nanotube composite membranes in which MWCNT were grown on alumina-polyamide (PA) template by CVD method. They investigated the experimental conditions (carbon precursor, temperature, deposition time) on the CNTs growth process. They successfully grew pure and catalyst free CNTs inside the alumina pores by CVD. [45] Hamed Parham et al reported thermal pyrolysis technique for the in-situ growth of CNTs-containing porous alumina structures. Carbon nanotubes were grown inside alumina matrix by heating at 850 °C using a catalyst [Ni $(NO_3)_2$] and a carbon source (camphor) [46]. They employed the same technique to develop ceramic CNTs composite filter for the removal of yeast and heavy metal ions. The filter mainly consisted of alumina and silica having pore size 300-500 µm and showed high efficiency

for yeast filtration (98%) and heavy metal ions removal (~100%) from water. [47] Ihsanullah et al reported the fabrication of silver doped CNTs membrane through powder metallurgical method. The MWCNT were compacted (200 MPa) and sintered (800 °C for 3 hours) after impregnation with silver through wet chemistry technique. The synthesized membranes were used to remove bacteria from water and 10% silver doped CNTs membrane showed 100 % bacterial removal in 60 min [48].

SPS is preferred to the conventional sintering techniques, due to the simultaneous application of pressure and temperature, enabling higher heating rate and shortening the sintering time as compared to conventional sintering. Therefore, SPS could be used to obtain higher strength at a lower temperature in comparison with hot pressing [49], and conventional sintering [50]. The porosity and strength of the membrane is controlled by SPS parameters [51]. SPS technique was reported to be promising for synthesizing the porous ceramics [52]. Improvement in the performance and reliability of the porous structures was reported via control pore geometry [53]–[57]. To our knowledge, the powder metallurgical technique was not reported in literature for the fabrication of CNTs-based ceramic composite membrane. Therefore, we decided to explore this area for developing porous alumina-CNTs nanocomposite membrane.

In the present study, powder metallurgical route was utilized to develop porous alumina-CNTs nanocomposite membrane by conventional solid-state as well as SPS. The composite powder mixture was initially prepared then compacted through uniaxial pressing followed by consolidation using pressure-less conventional sintering. The same mixture powder was also used to consolidate the membrane through spark plasma sintering (SPS). The effect of process parameters (sintering temperature, compaction load, heating rate and holding time)

on the overall performance of the membranes (% porosity, water permeability (or flux), and mechanical strength) was investigated. The best combination of process parameters was selected with the correlation of porosity and strength. Finally, the individual adsorption capacity of the constituent materials (alumina and CNTs) was studied for heavy metal (cadmium) through the batch experiments. The prepared membranes were then utilized to remove the Cd^{+2} ions form contaminated water in a flow loop system.

1.2 Aim/Objectives

The aim of this study is to develop and characterize porous alumina-CNTs nanocomposite membranes that can remove heavy metals, by physical adsorption, from aqueous solution. The specific objectives are as follows:

- To develop porous alumina-CNTs composite membranes using powder metallurgy technique
- To characterize the microstructure, properties and porosity of the developed membranes
- To evaluate the performance of the developed membranes for heavy metal removal (Cd^{+2} ions) from aqueous solution

1.3 Organization of the thesis

Chapter 1 introduces the topic and objectives of the work.

Chapter 2 contains a literature review about heavy metal removal techniques, particularly adsorption and membranes filtration. Adsorption capacity of various materials including alumina and carbon nanotubes (CNTs) and their comparison. Various methods to prepare and characterize the membranes.

Chapter 3 provides details about the materials and experimental procedures. Specifications of the materials used in the experimental work, and powder mixing methodology. Powder consolidation techniques and their process parameters

Chapter 4 contains the results and discussion obtained from the synthesis and characterization of the membranes (prepared by two different consolidation techniques) such as porosity measurement, diametrical strength, water permeation tests, microstructural analysis and finally a correlation of the results was made to obtain best combination of the strength and porosity. Moreover, the performance of the developed membranes against heavy metal (cadmium Cd^{+2}) removal is presented.

Chapter 5 includes the conclusions and recommendations

CHAPTER 2

LITERATURE REVIEW

Water is essential for life to exist and very important natural resource on the planet for all living things. Owing to the changes in the global climate and due to human interruptions in the ecosystem, water has started to loss its purity. Effluents, discharged from the industries (containing heavy metals), are polluting our lakes, rivers and under water resources. Toxic nature of heavy metal ions is very much established and well known in the present era. Metals do not decompose like biological matter but transform into various simple (atomic, ionic) or complex forms such as ligands or organometallic compounds. There are about 20 metals or like species that have proven to be toxic for human health. After the World War II, various committees had been formed and they published the maximum allowable concentrations (MAC) of the chemicals used in the industries which were the root cause of heavy metal exposure into the environment. Humans may either meet the metallic pollution by inhalation, ingestion or physical contact or due to their own interruption to the ecosystem through mining, melting, smelting, catalysis, fuel combustion, and production of semiconductors, superconductors, metallic glasses, alloy steels, nanotechnology. (monitored by International Agency of Research on Cancer, IARC, 2006). [58], [59]

2.1 Sources of heavy metal ions

Many industries producing huge amount of effluents that contain significant weightage of heavy metals in them. Some of these industries that discharge such pollutants into the

environment are given in table 2-1. [60] Most of the effluents discharged by these industries is toxic and cancer causing. Basically, three different types of pollutants that are considered hazardous to the environment are given bellow: [60], [61]

Toxic metals (such as Hg, Cr, Pb, Zn, Cu, Ni, Cd, As, Co, etc.)

Precious metals (such as Pd, Ag, Au, etc.) and

Radionuclides (such as U, Ra, Am, etc.)

Table 2-1: Industries producing heavy metals [60]

Melting and smelting industries
Surface finishing industries
Energies and fuel production industries
Fertilizers and plastic industry
Metallurgy (Iron and steel making)
Electroplating and electrolysis
Leather working (tanneries)
Photography
Aerospace industries
Atomic energy installations
Electric appliance manufacturing industries

2.2 Hazards associated with heavy metals

The term 'Heavy metals' is used to describe a group of metals with density greater than 5 g/cm^3 and atomic number above 20. However, any toxic metal can be considered as heavy metal irrespective of its mass and density. These elements are biologically toxic and considered pollutants to the environments. Many contaminants come under this category but the most common ones, with their maximum contaminant level (MCL) and associated ailments, are enlisted in Table 2-2. [62]

Table 2-2: Health risk associated with heavy metals & MCL standards [62]

Heavy metal	Toxicities	MCL (mg/L)
Arsenic	Skin manifestations, visceral cancers, vascular disease	0.05
Cadmium	Kidney damage, renal disorder, human carcinogen	0.01
Chromium	Headache, diarrhea, nausea, vomiting, carcinogenic	0.05
Copper	Liver damage, Wilson disease, insomnia	0.25
Nickel	Dermatitis, nausea, chronic asthma, coughing, human carcinogen	0.2
Zinc	Depression, lethargy, neurological signs and increased thirst	0.8
Lead	Damage the fetal brain, diseases of the kidneys, circulatory system, and nervous system	0.006
Mercury	Rheumatoid arthritis, and diseases of the kidneys, circulatory system, and nervous system	0.00003

2.3 Need to remove heavy metals

Pollutants, including heavy metals, are discharged into the freshwater lakes and rivers from industries, agricultural and domestic sources. These pollutants not only deposits into the sediments but aquatic life comes into direct contact with heavy metals. These heavy metals are non-biodegradable in nature and accumulate into aquatic organisms such as fish, oysters, mussels etc. Hence, they enter the food chain. Excessive amounts of these heavy metals are toxic to aquatic organisms as well as human beings. People eat contaminated food or drink water from the polluted source and finally exposed to metallic pollution reported all over the world. Owing to these toxic effects of heavy metals on the environment, organisms, and human beings, it is needed to remove them from the ecosystem. [63], [64]

2.4 Conventional techniques for heavy metal removal

As it is necessary to avoid the direct exposure of heavy metals to the organisms, it is needed to treat the wastewater before drain into the environment. Many physical, chemical and biological methods have been proposed and are in progress to mitigate the influence of these pollutants in the aquatic ecosystem. These methods are given below: [65]

- Chemical Precipitation
- Liquid-liquid Extraction
- Adsorption
- Membrane Filtration
- Ion-exchange
- Electrochemical treatment
- Reverse osmosis
- Evaporation recovery

Some of the above techniques are expensive while some are less effective to carry out. Some produce by-products that are difficult to process while some have limitations to employ in large scale. Although every technique has its own advantages and disadvantages but its use for heavy metal removal depends ultimately on economic and technical basis. However, adsorption and membrane separation are considered as popular and promising method for heavy metal removal among the conventional techniques because it is simple, easy to carry out and highly efficient. [65], [66]

2.5 Adsorption

In adsorption, adsorbates (species to be adsorb such as heavy metal ions) adhere and form film on large surface area of the adsorbents. Adsorbents (agents that adsorb or capture the

desired species from liquids or gases) with small particle sizes show large surface area for adsorption as well as better mass transfer efficiency. Fu and Wang reviewed 185 scientific publications in 2010 to discuss the most commonly used methods for heavy metal removal from wastewater. They concluded from the literature survey that adsorption, ion exchange and membrane filtration are the most frequently used techniques for heavy metal removal. [67]

2.6 Conventional Adsorbents

Activated carbon (AC) based absorbents fascinated the researchers worldwide because of their large micro-pores and high surface area for adsorption and thus had been used most commonly for capturing heavy metal ions from polluted waters. However, the depleted resources of coal based AC has increased its cost and made it difficult to use on commercial bases. Therefore, researchers are trying to add various new additives in AC to prepare cost effective and efficient composites. They are also trying to prepare new low cost materials for effective removal of heavy metals. [68]–[71] Various modified natural adsorbents (natural zeolite, modified clay, orange peel etc.), synthetic adsorbents (alumina, synthetic zeolite, clay-polymer composites, calcined/activated phosphates etc.), agricultural adsorbents (maize cope, rice husk, coconut charcoal, pecan shell activated carbon) or biological adsorbents (Spirogyra, marine alga and bacterial biomass etc.) had also been studied for adsorption of desired contaminants for water and wastewater treatment. Moreover, some industrial waste by-products (fly ash, waste slags, titanium oxide etc.) were also studied due to the economic benefits. [72]–[74]

2.7 Adsorption through alumina

Porous ceramics are very well known for their wide range of applications in many fields such as ionic conductors, adsorbents, membranes for filtration process. One of the very commonly used porous ceramic substrate for membranes is alumina. Alumina is a classic material not only to use as adsorbent but also to build membranes as well as supporting substrate for delicate membranes. It has large surface area for adsorption shows high adsorption capacities, good thermal stability, adequate mechanical strength. It can also be used as matrix for making composites with improved properties. [38], [75]–[81]

The adsorption properties of activated alumina and magnetic properties of iron oxide can be combined to develop magnetic alumina nano composite (MANC). A batch experiment was conducted to examine the feasibility of MANC to remove Cd^{+2} from the aqueous solution. The effect of pH, temperature, adsorbent dose, initial concentration and contact time was studied. The equilibrium data was fitted to the Langmuir, Freundlich and Temkin Isotherms. The MANC was characterized by XRD, SEM, TEM, EDX and BET. The thermodynamic data showed that adsorption was endothermic in nature. [82]

Surface complexation model (SCM) is commonly used to explain the adsorption of metal cations on the oxide surfaces. Various interpretations of adsorption have been used in different reviews [83]–[85] explain the adsorption details. The heavy metal cations are used to adsorb on the surface plane [86], [87]

$$Al\text{-}OH + Cd^{2+} = Al\text{-}OCd^{+} + H^{+} \qquad \text{(Eq. 4.1)}$$

Cadmium adsorb in the form cation. One proton is released as per one cadmium cation is adsorbed as shown in equation-4.1. However, adsorption of anionic cadmium chloride

complexes is negligible even the surface is positively charged and anionic complexes present in the solution. [88]

Yabe and Oiveira conducted a comparative study to investigate the adsorption capacities of sand, silica, coal and alumina for metal removal. Many heavy metals such as Pb, Cd, Ca, Mn, Mg, Fe, Zn, Ni, Cr and Cu were examined. After the adsorption process, the concentrations of Pb, Cd, Ni, Cr and Cu were found to be lower than the detection limit while for other metals the adsorption was low. The adsorbent to adsorbate ratio and contact time were determined to indicate maximum metal removal. [38] Alumina was found the best adsorbent solid and showed high adsorption efficiency to remove Fe, Cr, Pb, Ni, Cu, and Zn at 4 g/L in 5 min time. Fir. 2-1 shows a comparison of different adsorbents to remove heavy metals from the effluent.

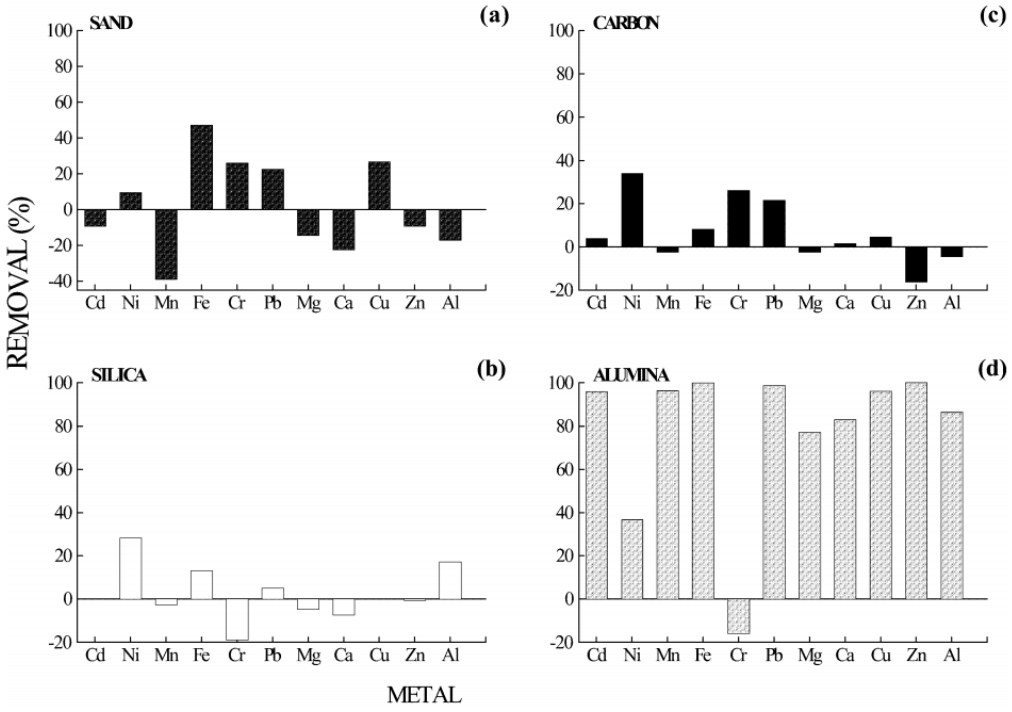

Figure 2-1: Comparative study of different adsorbents (alumina, carbon, silica, and sand) for various heavy metals [38]

Sharma et al synthesized nano alumina particles by sol-gel method and found that the removal of Ni^{+2} from the aqueous solution was dependent on the initial concentration, adsorbent dose, pH and temperature. [75] Adsorption increased with increasing pH from 2 to 8. Maximum removal achieved at PH 8. Temperature also influenced the adsorption process a bit and removal increased (97-99%) with increasing the temperature from 25 to 45 °C. In the end, the adsorption capacity of the manufactured nano alumina was compared with other adsorbents as shown in Table 2.3.

Table 2-3: Comparison of Alumina with other adsorbents [75]

Adsorption	adsorption capacity (mg/g)	references
Bagasse	0.001	32
fly ash	0.03	32
Aspergillus niger	1.1	33
granular activated carbon	1.5	7
sheep manure waste	7.2	34
peat moss	9.18	35
coir pith	9.5	4
calcium alginate	10.5	36
baker's yeast	11.4	3
Thuja orientalis	12.42	9
carbon aerogel	12.87	37
waste tea	18.42	10
Fe(III)/Cr(III) hydroxide	22.94	38
Nano-alumina powder	30	Present study

2.8 Adsorption through carbon nanotubes (CNTs)

In recent times, water treatment through nanomaterial has gain its importance due to the unique properties associated with nano-sized materials. Nanomaterials show high surface area and larger interactive sites for metallic species. Moreover, their efficiency can be increased by attaching functional groups to their surfaces that in turn increase the number of active sites for capturing more and more contaminants. [89]–[92]

In 1991, Ijima discovered a new member of carbon family (carbon nanotubes, CNTs) that showed great potential as nano adsorbent for its unique properties. After considerable research on this new adsorbent, it is now proven that CNTs have great potential as contaminant adsorbent. CNTs are of two types, single walled (SWCNTs) and multi-walled (MWCNTs) as shown in Fig 2-2. [93], [94]

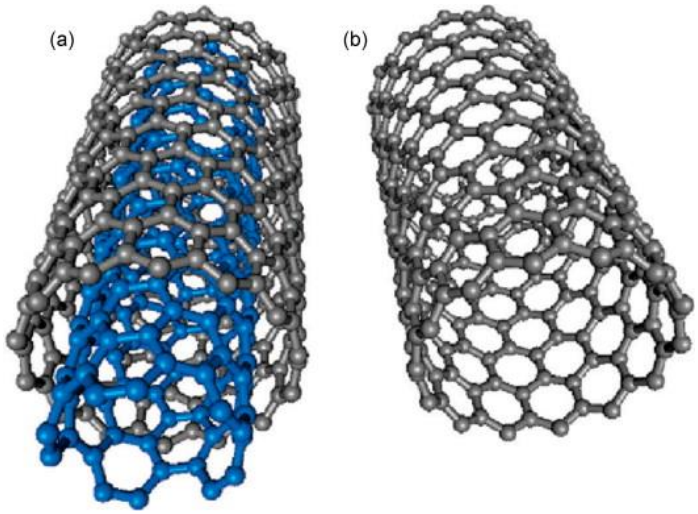

Figure 2-2: (a) MWCNTs (b) SWCNTs [60

If we compare adsorption properties of CNTs with that of AC (most commonly used material for heavy metal removal), we came to know that CNTs are way better than AC because of its large specific surface area, high porosity, light mass density, regular structure at nano level and strong interaction between metal ions and the CNT surface. Researchers have studied the adsorption behavior of small molecules, heavy metal ions, organic molecules and radionuclide on the single walled, multi walled, open and close-end CNTs. Following four factors are important while studying the adsorption behavior of CNTs: [95]

I. The number of active and contributing sites in the adsorption process is very important. It is possible to know the number of adsorption sites through temperature

programmed desorption mechanism. However, there are four different sites on the CNT bundle to capture the desired species as shown in Fig 2-3. [96], [97]

1. Interior sites of every individual tube and these tubes are only exposed when caps are removed from the tubes.
2. Channels between the tubes of the interstitial sites.
3. Groove produced in between two adjacent tubes
4. The curved outer surface of the tube in nano bundles.

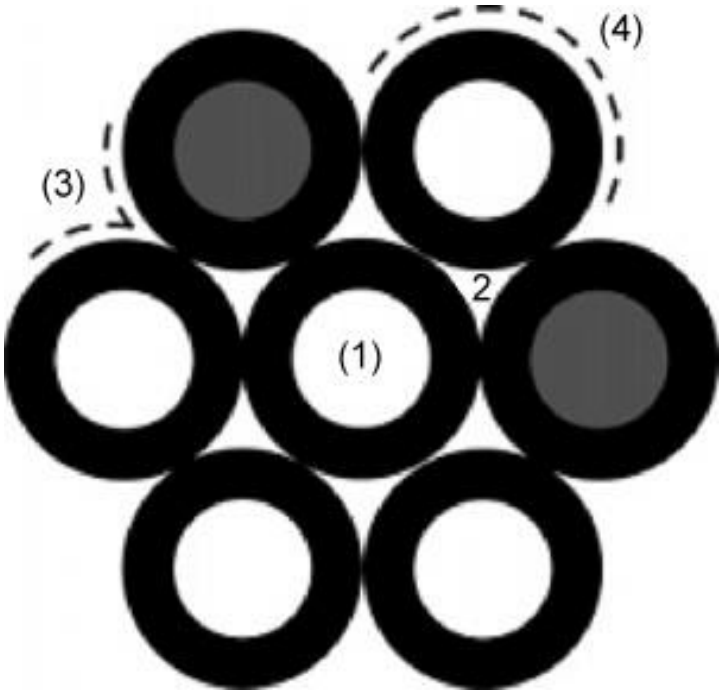

Figure 2-3: Four possible adsorption sites on the nano bundle [63]

Extensive study has been done to find out where and how the adsorbing species attach on the nanotubes. For close-end CNT, adsorption usually takes place at grooves because of the easy access to the exposed surfaces. While in the case of open-end CNTs, adsorption process starts from the outer surfaces followed by internal wall saturation of the tubes. [98]

II. The amount of uncapped or open-ends in the CNT bundles considerably influence the adsorbing behavior of nanotubes. More the open ends on the nanotube surfaces, more the adsorption take place. [99]

III. Usually, impurities are found embedded on the surface of the nano bundles that may be an adsorbent on their own, hence, distort the adsorbing behavior of CNTs. Moreover, these impurities cover the CNT bundles and reduce its adsorption capability. [100]

IV. Several functional groups or oxygen content on the nanotube surfaces influence the adsorption behavior of CNTs. Total oxygen content on the CNT surface (oxygen functional groups: -OH, -C=O, -COOH) influence the adsorption capacity of the nanotubes. Usually higher the oxygen content, higher will be the adsorption capacity of the CNTs. These functional groups can be introduced to the CNT surface by oxidation using either of the following methods:

    1. Various Acids [101], [102]

    2. Ozone [103]–[105]

    3. Plasma [106]

pH is also an important factor in adsorption of heavy metal cations on the CNTs surfaces. The adsorption of cations is higher if the Ph value is than pH_{pzc} because of electrostatic attraction between the cations and the negatively surface charge. However, at lower pH the adsorption decrease due to charge neutralization. The changing pH also affects the competing complexation reactions. Hence, the adsorption capability of CNTs changes with change in pH values. [107], [108] The pH_{pzc} of raw CNTs is in the range of 4-6 [109], [110] while acid treated CNTs were reported to have lower pH_{pzc} as compared to raw CNTs. [111] The state of divalent metal ions in solution depends of the pH and most commonly produced species are M^{+2}, $M(OH)^{+}$, $M(OH)_2$, $M(OH)^{3-}$ [107], [112], [113]. The proton release reaction by CNTs is shown below [107]

$$\text{CNT-OH} + H^{+} \leftrightarrow \text{CNT-OH}^{2+}$$
$$\text{CNT-OH} \leftrightarrow \text{CNT-O}^{-} + H^{+} \qquad \text{(Eq. 4.2)}$$

The adsorption of mechanism of divalent metal ions onto CNTs is shown below

$$\text{CNT-OH}^{2+} + M^{2+} \leftrightarrow [\text{CNT-OHM}^{+2}]^{+2} + H^{+}$$
$$\text{CNT-O}^{-} + M(OH)^{2-n} \leftrightarrow [\text{ CNT-O-M(OH)}^{2-n}] \qquad \text{(Eq. 4.3)}$$

The heavy metal ions are adsorbed on the surface of the CNTs due to competition between M6 and H6+ in the solution. However, if the pH value is higher than pH_{PZC}, the dominant divalent species on the solution is $M(OH)^{2-n}$.

Fig. 2-4 showing the mechanism of functional group generation on CNT by using plasma technique. These functional groups can be removed intentionally by heat treatment. [114] Heavy metal adsorption capacity of raw CNTs is considerably small but can be increased

when their surfaces are oxidized through HNO3, NaClO, or KMnO4 solutions. Lu et al modified the surface of CNTs by using these chemicals and found that adsorption properties of CNTs increased for toluene, benzene and BTEX after oxidizing them with the chemicals [115]

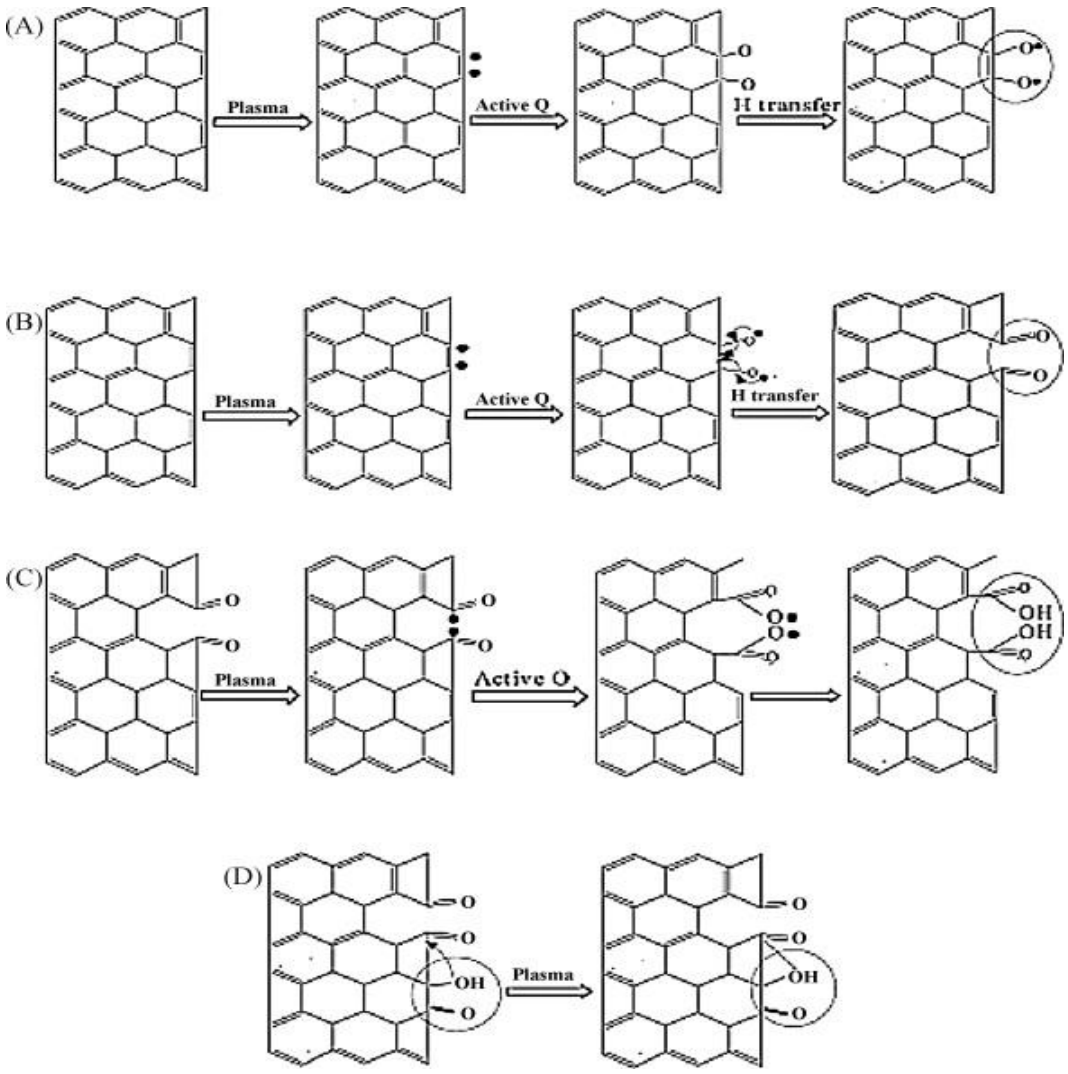

Figure 2-4: Plasma technique to generate FG on CNT surface [115]

It is proven from the study that CNTs have great potential to adsorb heavy metal ions such as Cd^{2+}[116], Cu^{2+}[117], Ni^{2+}[118], Pb^{2+}[119], Zn^{2+}[120], Fe^{3+}[121]. The adsorption on

CNTs is strongly influenced by the value of pH. Under similar conditions adsorption capacity of CNTs is higher than that of other adsorbents. Table 2.3 shows a comparison of adsorption capacities of various adsorbents at various pH values. [122]

Table 2-4: Comparison of adsorption capacity of CNTs & other adsorbents for heavy metals [122]

Adsorbates	Adsorbents	Q (mg/g)	Conditions
Pb(II)	Acidified MWCNTs	49.71	pH 5.0, T 298 K
	Native bentonite	19.19	T 303 K
	Cicer arientinum biomass	27.79	pH 4.0, T 303 K
	Pine wood char	4.13	pH 5.0, T 298 K
	Activated carbon F-400	30.11	pH 5.0, T 298 K
Cu(II)	As-produced CNTs	8.25	pH 6, T 300 K
	NaOCl-modified CNTs	47.39	pH 6, T 300 K
	Activated carbon	19.50	T 303 K
	Sawdust	37.17	pH 6.6, T 303 K
	Zeolite	8.13	pH 5.0, T room
Ni(II)	MWCNTs	3.72	pH 5.4, T 293 K
	NaClO-modified SWCNTs	47.86	T 298 K
	NaClO-modified MWCNTs	38.46	T 298 K
	Granulated activated carbon	2.88	pH 4.5, T 298 K
	Montmorillonite	12.89	pH 6.0, T 298 K

The mechanism of heavy metal adsorption on the surface of the CNT is attributed to

1. Physical Adsorption
2. Electrostatic Attraction
3. Precipitation
4. Chemical interaction between metal ions and CNT's surface functional groups

Among the above said mechanism chemical interaction between metal ions and the functional groups is the major adsorption mechanism as shown in Fig. 2.5. [123]

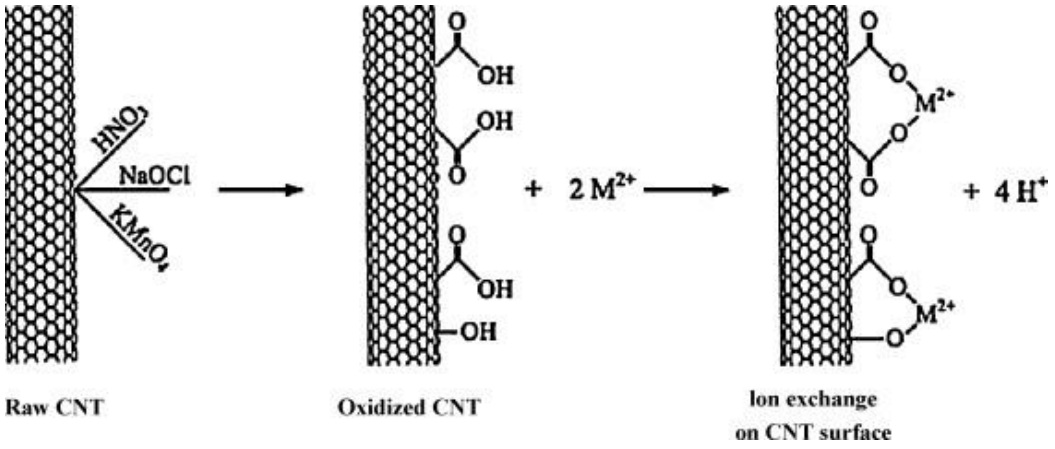

Figure 2-5: Chemisorption of metal ions by functional groups present on CNT surface [123]

A comparison of raw MWCNTs and surface acidified MWCNTs, with various chemicals, was made to adsorb Pb (II) ions. It was fond that adsorption capacity increased after oxidizing the surfaces of the MWCNTs. The results showed that 75.3% adsorption of Pb ions was carried out on the functional groups while the contribution of the physical adsorption (depends on surface area, defects, and open ends) was about 24.7%. [124] It came to know that metal ion sorption capacity of CNTs does not largely depends on the surface area, pore volume and mean pore diameter but strongly depends on surface total acidity. Sorption of metal ions on activated CNTs increases with CNT mass, contact time, and temperature while decreases with increasing ionic strength of the solution. Enthalpy change for sorption is positive which indicate the endothermic nature of sorption. The pH phenomenon is also very important for studying the sorption process as the solution pH drops after sorption takes place. This is because of the release of the protons from the functional groups on the CNT surface to capture metal cations. [119], [125]

Fig. 2-6 demonstrated the possible interaction mechanisms of cadmium ions adsorption on CNT/ Al_2O_3 surface. Cadmium ions are adsorbed on the surface modified CNTs via

physical interactions, electrostatic interactions and van der Waals interactions occurring between the Cd(II) ions and hexagonal arrays of carbon atoms in the folded graphite sheet [126].

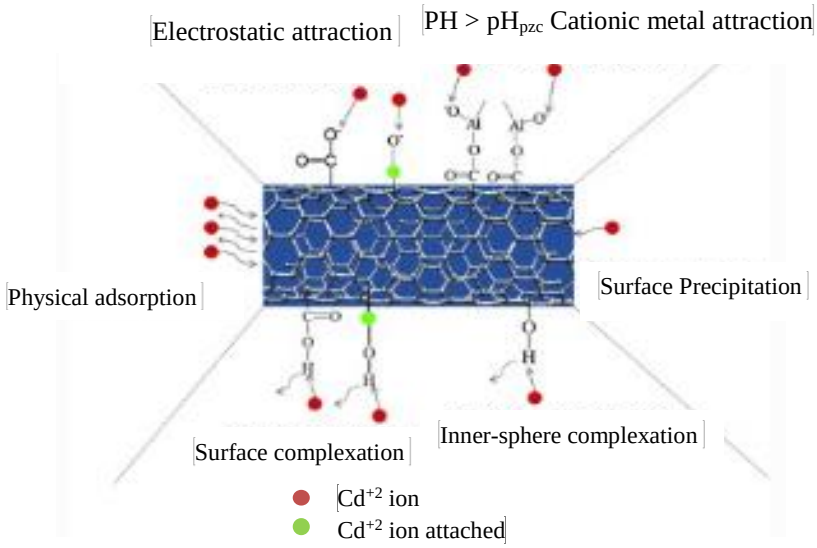

Figure 2-6: Schematic of the possible mechanism of cadmium ion adsorption on CNT/Al2O3 surface [126]

Acid modified CNTs have higher removal efficiency for heavy metals than raw CNTs [67]. However, the adsorption mechanism of different metal ions on CNTs is not the same and the affinity order of metals ions towards CNTs is different. Stafiej and Pyrzynska [110], reported that the affinity order of the certain metal ions towards CNTs is $Mn^{2+} < Zn^{2+} < Co^{2+} < Pb^{2+} < Cu^{2+}$ at pH 9. In two other studies, the following affinity orders were reported: $Pb^{2+} > Cd^{2+} > Co^{2+} > Zn^{2+} > Cu^{2+}$ and $Cd^{2+} < Cu^{2+} < Zn^{2+} < Ni^{2+} < Pb^{2+}$ [127]. These results suggested that the adsorption of heavy metals on CNTs depends mainly on the properties of CNTs.

2.9 Separation through CNT-based composite membranes

Hsieh and Hong grew CNTs on alumina particles for adsorption of heavy metals from the solution and compared the results with AC powders, commercial CNTs, and alumina

particles. They claimed to obtain extraordinary adsorption results by using oxidized CNTs on alumina that were superior to other adsorbents. The preference order of adsorption was given as $Pb^{2-}>Cu^{2+}>Cd^{2}$. The adsorption calculation of 1 g of CNTs on Al_2O_3 was 67.11, 26.59, and 8.89 mg/g for Pb^{2-}, Cu^{2+}, and Cd^{2+} in single adsorption test, respectively. [128] Tariq Altalhi et al [62] grew MWCNTs by chemical vapor deposition (CVD) on the template of nano porous alumina membrane as shown in fig. 2.7. The transport properties of the membrane were investigated by diffusion of dye (Rose Bengal model).

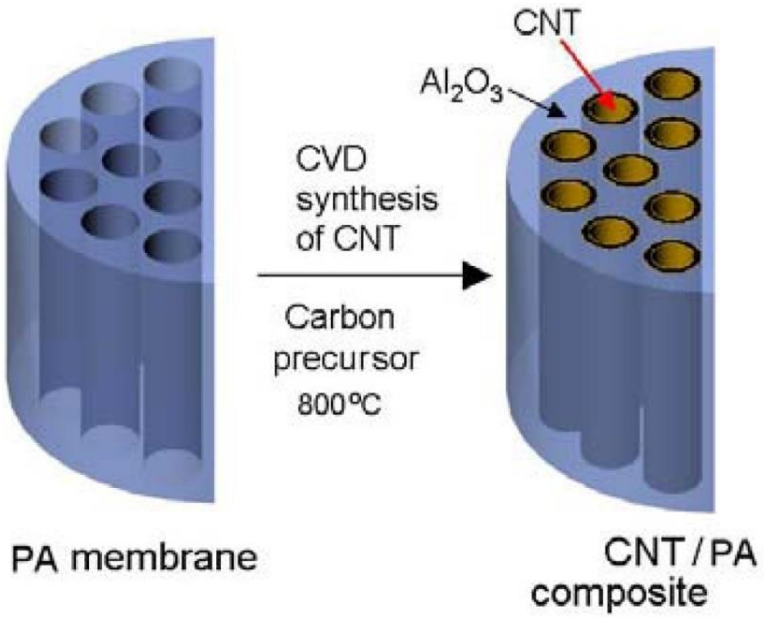

Figure 2-7: Schematic of CNT/PA membrane developed through CVD growth of CNTs inside the alumina pores [62]

Vertically aligned CNTs were grown by using catalyst precursor on the porous alumina substrate by CVD method for gas permeation as shown in figure 2-8. [129] Lee et al also developed vertically aligned CNTs membranes for water purification that showed very

high water permeability 30,000 L. $m^{-2}.h^{-1}.bar^{-1}$ as compared to previously known value 2400 L. $m^{-2}.h^{-1}.bar^{-1}$. [130]

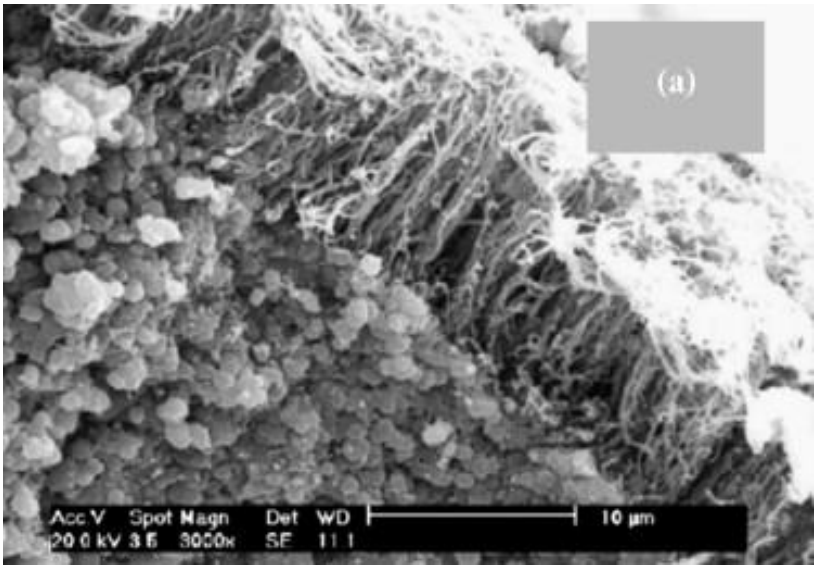

Figure 2-8: Vertically aligned CNTs on alumina template [129]

Hamed Parham et al reported thermal pyrolysis technique for the in-situ growth of carbon nanotube-containing porous alumina structures as shown in figure 2-9. Carbon nanotubes were grown inside alumina matrix by heating at 850 °C using a catalyst [Ni $(NO_3)_2$] and a carbon source (camphor) [46]. They employed the same technique to develop ceramic carbon nanotube composite filter for the removal of yeast and heavy metal ions. The filter mainly consisted of alumina and silica having pore size 300-500 µm and showed high efficiency for yeast filtration (98%) and heavy metal ion removal (~100%) from water. [47]

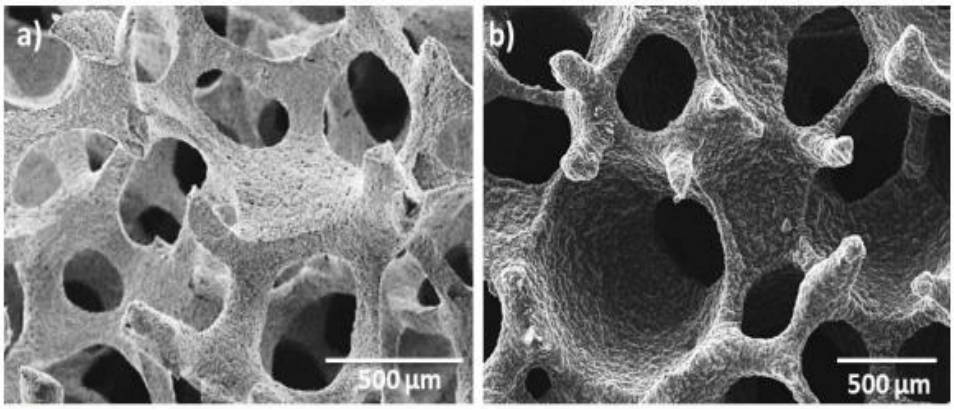

Figure 2-9: FE-SEM images of porous alumina matrix (a) before CNTs growth (b) after CNTs growth [46]

Tofighy and Mohammadi reported an adsorptive membrane (disk shaped) developed by growing CNTs randomly by CVD method on the mullite substrate as shown in figure 2-10. They used the prepared membrane for Ni ion removal from water. Fig. 2-11 shows that water flux values decreased considerably by growing the CNTs layer on the mullite surface and the maximum Ni ion rejection achieved was 63 %. [131]

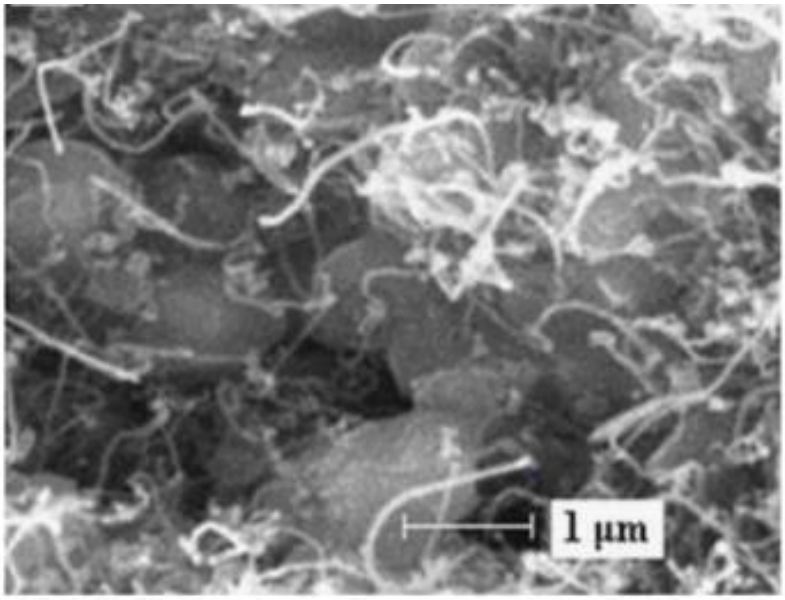

Figure 2-10: Randomly oriented CNTs on mullite substrate [131]

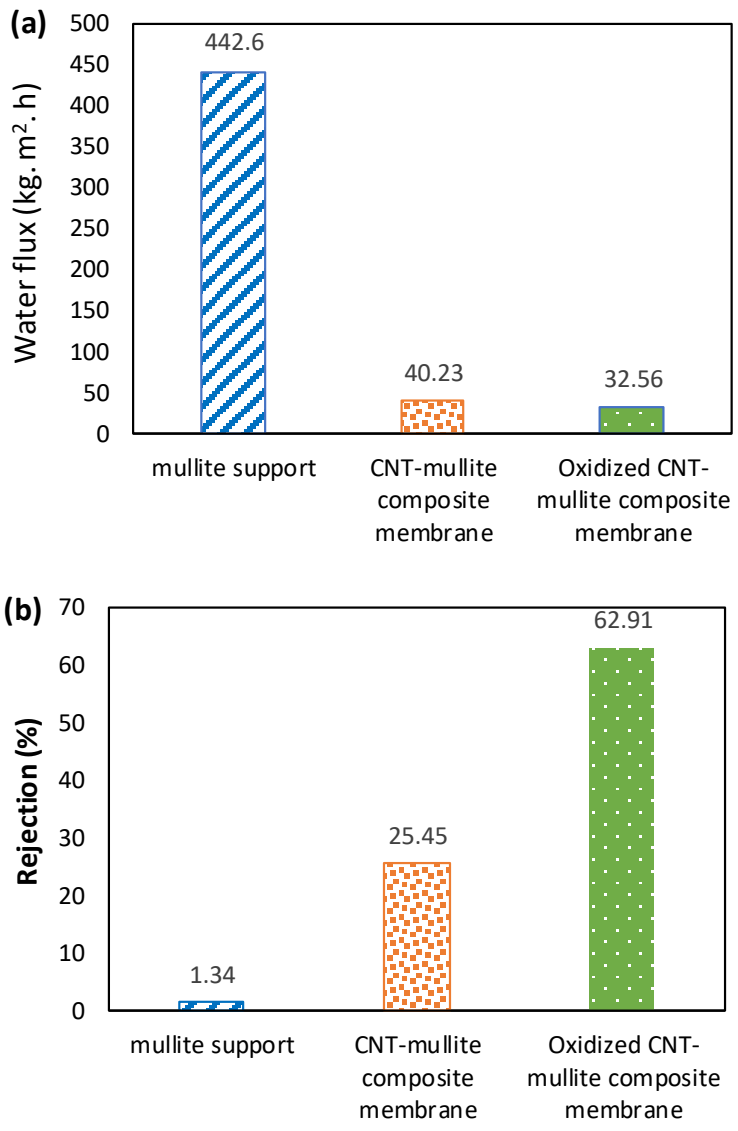

Figure 2-11: (a) water flux (b) Ni ion rejection from CNT-mullite membrane [131]

2.10 Powder metallurgical method to develop ceramic membranes

2.10.1 Pressure-less solid state sintering

Burma and Mandal worked on α-alumina membrane supports and investigated the effect of initial compaction load and sintering temperature on the quality of the alumina membrane support. They used dry compaction method to shape the membrane in disc form

followed by sintering. They used a range of compaction loads from 50 to 350 KN and a range of sintering temperature from 1200 C to 1500 C. They concluded that lower the sintering temperature and lesser the compaction load, more porous (porosity 55%) the alumina membrane achieved and vice versa. But the highest flexural strength (about 200 MPa) obtained at highest compaction load 350 KN and sintering temperature 1500 C. [132]
Wu Qin et al also used the same technique to prepare porous membrane support with the addition of boehmite with alumina and found the effect of boehmite and sintering temperature on the pore openings, pore sizes, and porosity. They mentioned the average pore size of the support as 5.1 µm with porosity about 53%. They also work on the mechanical strength of the supports and found the bending strength as 35.5 MPa. [133]
Korosh Shafieia et al designed disc type alumina microfiltration membranes and compared the relationship of binder type (CMC, PVA and Xanthan gum) and its amount (30g binder in 1-3 cm^3 of volume), compaction pressure (300-500 bars) and sintering temperature (1350- 1500 C) on the porosity of the membranes. However, they attained porosity up to 49% but membranes were delicate and crushed during water flux test. [134]
Lyckfeldt" and Ferreira discussed a similar method for porous ceramic processing consolidation. They used starch as binder and pore former in alumina to consolidate porous structure after sintering. [135]

Javad Ghaderi et al manufactured alumina membrane supports with vibration and compaction methods with or without the addition of silica. They tried to evaluate porosity, compressive strength and thermal conductivity of the membranes as a function of silica addition and sintering temperature. They end up with the conclusion that compaction load has a great effect on sintering and ultimately the properties of the samples. However, they

suggested that high porosity (50%) can be achieved at optimum sintering conditions (1475 °C) without using silica. [136]

Faheemuddin Patel et al studied different ceramic materials α-alumina, zirconia, and SiO_2. They reported their work in disc-shaped ceramic membranes support that was fabricated by uniaxial compaction of α-alumina powder followed by sintering at 1400 C. The comparative study was done and the effect of compaction load on the green density of the supports was evaluated. [25]

Tahar Laoui et al manufactured microporous alumina layer on porous zirconia substrate by suspension sedimentation method for filtration purpose. The deposition of a micro-porous layer on the substrate was evaluated using various chemicals (SDS, Triton-X, and citric acid). They concluded that SDS caused the deposition of a uniform layer with least agglomeration among other chemicals under examination. [137]

Ihsanullah et al [72] developed Ag-doped carbon nanotube membranes through powder metallurgical method. Carbon nanotubes were first impregnated with nano silver particles with different loadings using wet chemistry technique followed by compaction into disc shaped membranes. These compacted membranes were sintered at 800 °C. They characterized the membranes and found that membranes possess strong antibacterial properties with good water permeation flux. So, these membranes are usable for continuous filtration process and can be used to remove various types of contaminants. [48] Further to the previous work, Ihsanullah et al impregnated the carbon nanotube with iron oxide this time with different loadings and evaluated its anti-fouling properties using sodium alginate. The maximum removal of SA achieved through the membrane was 90%. [138]

2.10.2 Spark plasma sintering

SPS is preferred to the conventional sintering techniques, due to the simultaneous effect of pressure and temperature, enabling to higher heating rate and shortening of the sintering time, and less temperature as compared to conventional sintering. This helps to get fine pores formation. Moreover, SPS could help to get higher strength at a lower temperature in comparison with hot pressing [139], and conventional sintering [140]. In addition, the porosity of the membrane could be controlled by SPS temperature [24]. Therefore, SPS technique was reported to be promising for synthesizing the porous ceramics [52]. Moreover, improvement in the performance and reliability of the porous structures were reported via control pore geometry [141]–[145].

Chakravarty et al used spark plasma sintering (SPS) technique to produce high strength porous alumina supports. This technique is usually utilized to develop compacted and dense samples. However, they controlled the parameters (T= 1000-1200 C) and (P = 10-50 MPa) to get porous ceramic structure. The results showed that the porosity and bending strength were highly influenced by applied sintering pressure. [146]

From the literature review carried out on the topic, it is concluded that both alumina and CNTs powdered materials are good adsorbents of toxic heavy metals, particularly CNTs due to their remarkably high surface area. However, to our knowledge no prior work has been reported on the combination of both materials to fabricate alumina-CNTs nanocomposite membrane through compaction and sintering. Therefore, we decided to use conventional pressure-less and spark plasma sintering (SPS) methods to fabricate alumina-CNTs nanocomposite membranes in the current study.

CHAPTER 3

MATERIALS AND EXPERIMENTAL PROCEDURE

This chapter includes the detailed information about the materials, equipment and experimental procedure and characterization techniques used for research. Probe sonicator was used for homogeneous CNT missing with continuous magnetic stirring. The process parameters of SPS as well as pressure-less solid-state sintering were optimized for membranes' fabrication. The synthesized membranes later used for heavy metal (Cadmium) removal from contaminated water.

3.1 Materials

Alumina powder (α-alumina of 0.3-micron particle size) was procured from Buehler, Illinois, USA. Commercial multiwall carbon Nanotubes (MWCNTs) were purchased from Times Nano, Chengdu Organic Chemicals Co. Ltd. China, having purity >95%, OD: 10-20 nm and length: 10-30 µm. Poly Vinyl Alcohol (PVA) was used as a binder while Gum Arabic (GA) and Sodium Dodecyl Sulfate (SDS) were used as dispersants for CNTs and all of them were purchased from Loba Chemie Pvt. Ltd., Mumbai, India as shown in figure 3-1. For heavy metal removal tests, cadmium (Cd^{+2}) standard solution (1000 ppm) was purchased from Ultra-scientific USA.

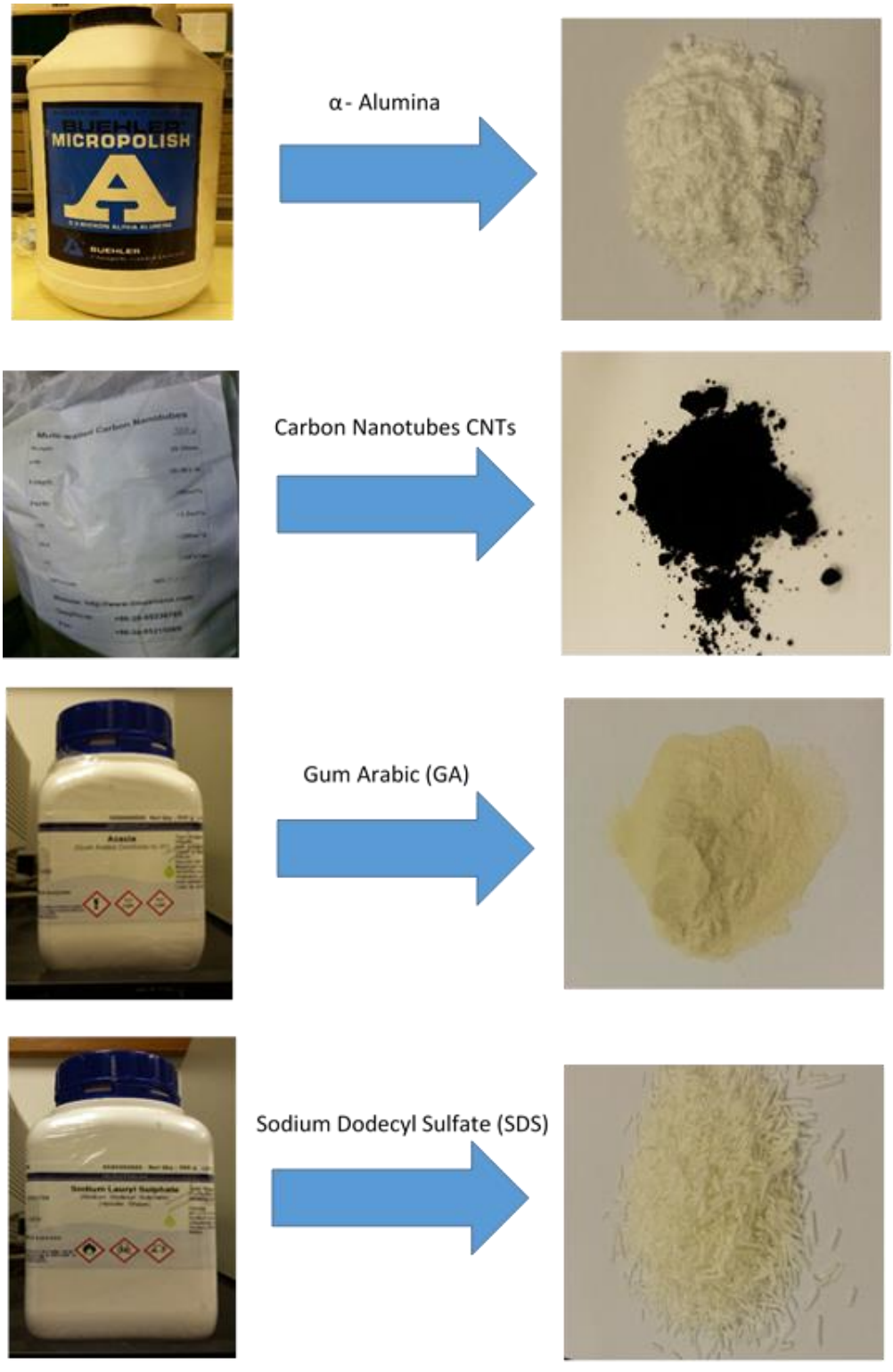

Figure 3-1: Raw materials used for powder mixture preparation

3.2 Experimental Procedure

3.2.1 Powder Preparation

Powder metallurgical process was used to produce alumina-CNT composite powder mixture (5% loading of MWCNTs were added into 95% alumina matrix.). Gum Arabic (GA) and Sodium Dodecyl Sulfate (SDS) were used in combination (1:1), as dispersants, to avoid Carbon Nanotubes agglomeration. [147]. All three components were dispersed and hand mixed in distilled water with dispersants (GA+SDS) followed by probe sonication for 1 hours.

Parallel to this work, another mixture (alumina + starch) was prepared. Starch (5% of the powder mixture) was used as a pore former in alumina matrix [135]. After One hour of sonication of the above CNT mixture, the powder mixture of alumina and starch was added into it. The whole mixture was sonicated again for 2 hours for good mixing of all the components homogeneously.

Afterward, water was evaporated from the mixture on a hot plate with continuous stirring. After getting the final mixture powder, 10 % binder solution (prepared by adding 2% PVA in distilled water) was added into it for better compaction [23]. Fig. 3-2 shows the flow chart of the complete mixture preparation process.

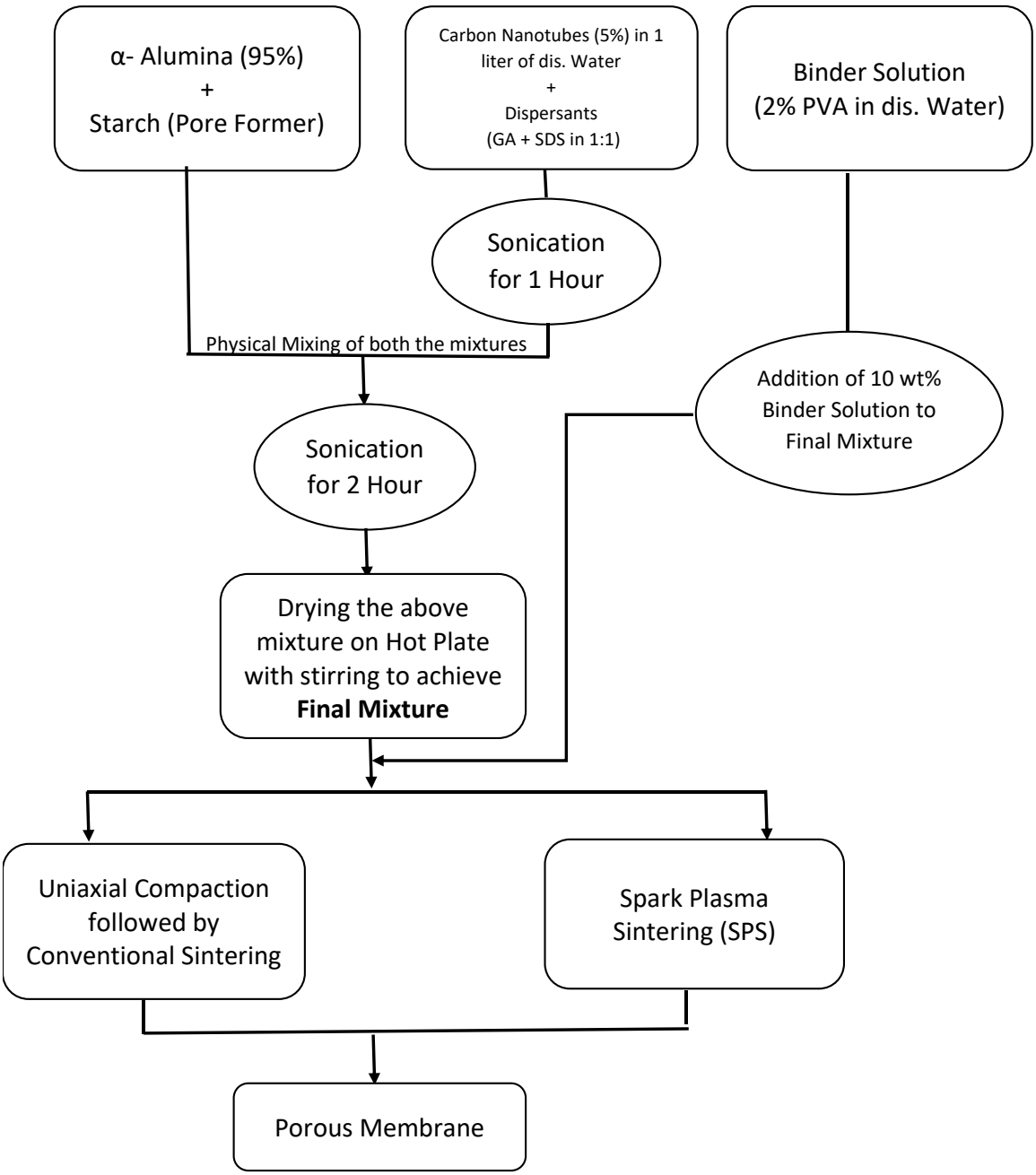

Figure 3-2: Flow chart representing alumina-CNTs membrane synthesis

3.2.2 Membrane synthesis by conventional pressure-less sintering

The alumina-5%CNT powder mixture was then compacted into disc-shaped membranes. The compaction was done in a stainless-steel die (diameter: 27.5mm diameter) with the help of a uniaxial pressing machine (Wabash, Indiana. USA) as shown in figure 3-3. The compaction converted the powder mixture into a disc of 4mm thickness and 27.5 mm diameter.

Initially, the powder was compacted at 50 KN load with a dwell time of 2 minutes to achieve a porous green compact. [23] The compacted disc was then removed from the die by using hydraulic press (APEX London) and sintered at four different temperatures (1200°C, 1300°C, 1400°C, and 1500°C) in a tube furnace (GSL 1700X, MTI Corp. USA), as shown in figure 3-4, to evaluate the effect of sintering temperature on the properties of the final membranes. The heating rate of 5 °C /min was used throughout the heating cycle while holding time was 4 hours at 500 °C and then at the sintering temperature. In the second stage of the experimentations, the effect of compaction load on the porosity and mechanical strengths of the membranes were examined. This time, alumina-CNT nanocomposite mixture was compacted with increased compaction loads (100 KN, 150 KN, and 200 KN) and sintered at two different temperatures 1400°C and 1500°C (the temperatures that were optimized for the first set of experimentations) to get the optimum combination of strength and water porosity in the membrane.

Figure 3-3: Compaction process of alumina-CNTs powder mixture (a) custom-made stainless steel die for powder mixture compaction (b) compaction process using uniaxial pressing machine (c) sample removal from die after compaction using hydraulic press (d) aluimna-5%CNTs compacted sample

Figure 3-4: Pressure-less solid state sintering process (a) green alumina-CNT disks for pressure-less sintering (b) installing the samples into tube furnace for sintering (c) Tube furnace

3.2.3 Membrane synthesis by spark plasma sintering (SPS)

In addition to conventional pressure-less sintering technique, spark plasma sintering (SPS) method was employed to fabricate the porous alumina–CNT composite membranes. SPS machine (FCT system-model HP D5, Germany) was utilized in the present study to carryout membrane fabrication as shown in figure 3-5.

Figure 3-5: Spark plasma sintering (SPS) furnace (FCT, HP-D5, Germany)

3.3 Characterization Techniques

Various characterization techniques were used to analyze the properties of as received powders (alumina and CNTs), their mixture and finally the synthesized membranes.

3.3.1 X-ray diffraction (XRD)

X-ray diffraction (XRD) was performed using x-ray diffractometer (Bruker, D8 Advanced) with the scanning rate of 2°/min for 2 theta angle of 20° to 80° to analyze the structure of fabricated membranes.

3.3.2 Field Emission Scanning Electron Microscopy (FE-SEM)

Surface morphology and micro-structural analysis of the samples (average particle size, pore size, and a number of pores) was observed by Field Emission Scanning Electron Microscopy (FE-SEM) facility (TESCAN, Lyra 3).

3.3.3 Water Permeation Test

Water flux measurement was carried out with the help of a custom-made flow loop system as shown in Fig. 3-6. Pure water flux J (L**.** m^{-2}**.** h^{-1}) of the membrane through the transmembrane pressure (1-5 bar) were calculated using equation-1. [48]

$$J = \frac{V}{A \, . \, t} \qquad \text{(Eq. 3.1)}$$

Where A (m^2) is the membrane surface area, V (liters) is the volume of water passing through the membrane at a measured time t (h).

Water flux is generally a linear function of the transmembrane pressure. Higher the water pressure on the membrane, higher is the water transport through it and hence higher the

permeability. [48]. The same loop was further utilized to perform heavy metal (cadmium) removal analysis.

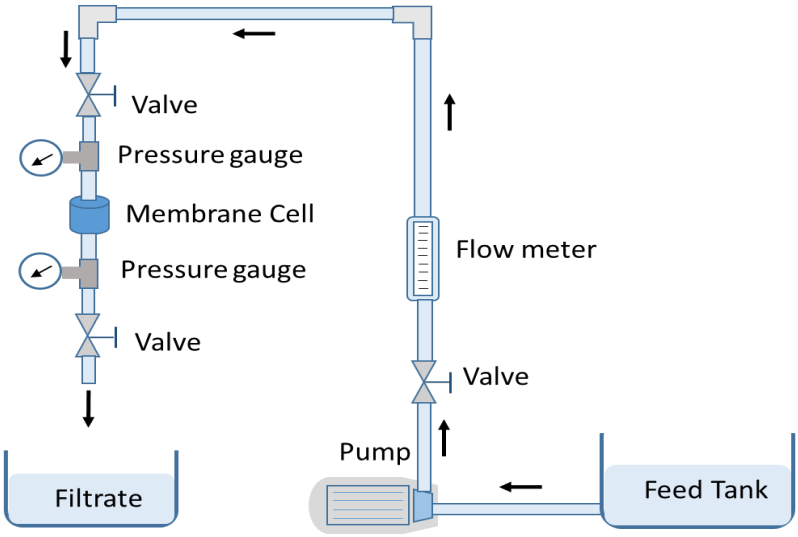

Figure 3-6: Flow loop system used for water flux measurement and heavy metal removal test

3.3.4 Porosity measurement

The porosity of the membrane was measured as per the ASTM standard for porous ceramic materials (ASTM c373-14a) [136, 148]. Wet and dry weights of the membrane were calculated as suggested in the standard to measure the percentage porosity of the membranes using equation-2.

$$V = M - S$$

$$P = \left[\frac{(M - D)}{V}\right] \times 100 \qquad \text{(Eq. 3.2)}$$

where, P is the apparent porosity, D is the dry weight, M is saturated weight, S is the suspended weight, and V is the volume of the membrane.

3.3.5 Diametrical compression test

The mechanical strength of the membrane was evaluated using diametrical compression test. A schematic of the test is shown in Fig. 3-7(a). This test was used to estimate the strength of porous ceramic membrane. [12] In this test, the membrane was placed in vertical position flat and tensile stresses are developed, within the membrane, perpendicular to the compressive load causing the sample to break into two pieces. The fracture propagation at the middle of the sample is an indication of successful completion of the test as shown in Fig. 3-7 (b). The test measures the strength of the membrane while load is applied diametrically using equation-3. [12], [149]

$$\sigma = \frac{2\,P}{\pi\,.D.t} \qquad \text{(Eq. 3.3)}$$

'P' is the applied load; 'D' is the diameter and 't' is the thickness of the membrane.

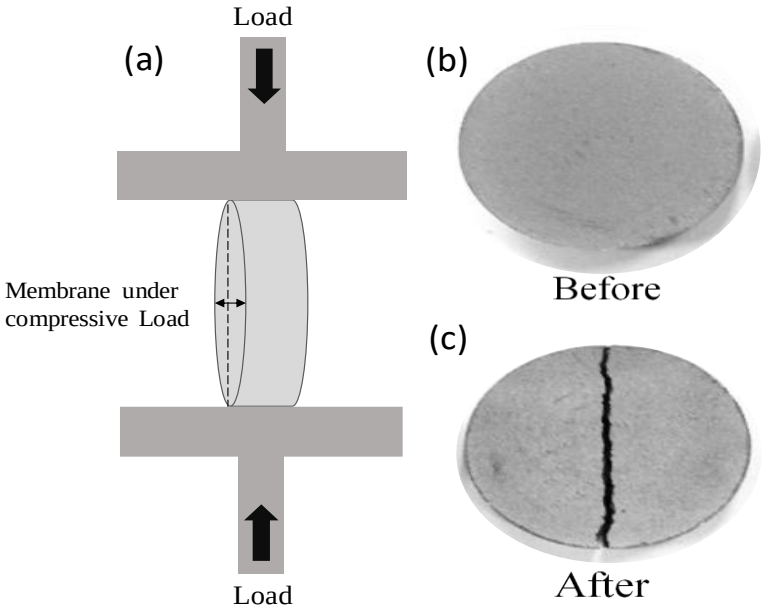

Figure 3-7: Schematic of diametrical compression test (b, c) Alumina-CNT membrane before and after the test

3.4 Heavy metal removal test

The batch adsorption analysis was carried out initially to evaluate the cadmium (Cd) removal efficiency of the individual and mixture powders. The 1ppm concentrated solution of cadmium was prepared using cadmium (Cd) standard solution (1000 ppm) supplied by Ultra-scientific USA. The powder suspension in (5g/L) was stirred on the orbital shaker for 1 hour with the speed of 150 rpm. Blank tests without cadmium were performed to evaluate the effect of sorption on container wall and precipitation. Three sets of each sample were prepared to get reliable results as shown in figure 3-8.

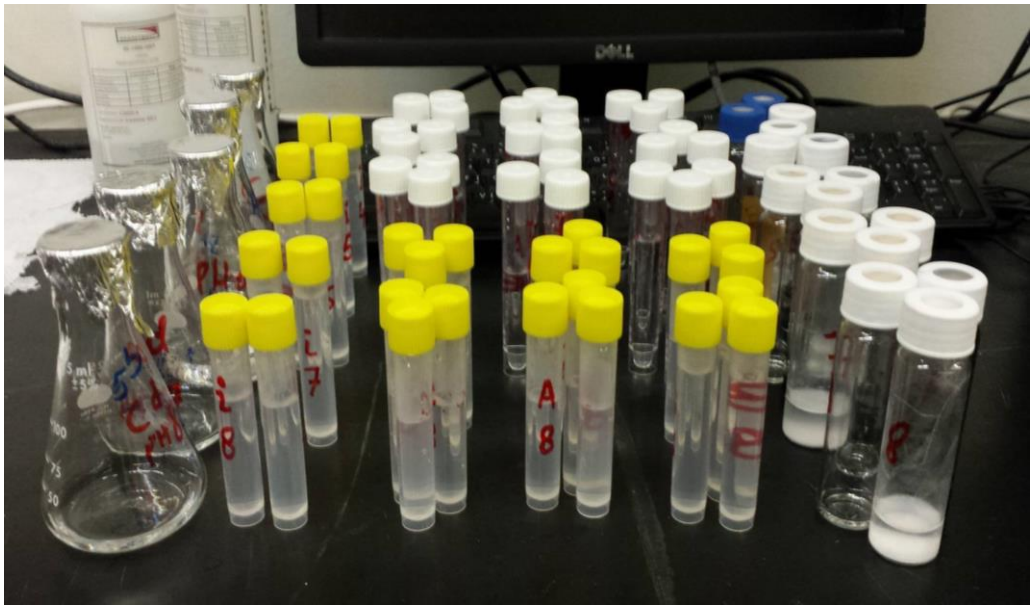

Figure 3-8: Samples prepared to carryout pH analysis during batch adsorption test

Later, adsorption capacity of the selected alumina-CNTs membrane was investigated. The analysis was carried out using flow loop system as shown in Fig. 3-6. The filtrate was collected after a single run through the membrane and analyzed using inductively-coupled plasma optical emission spectroscopy (ICP-OES) Optima-8000 as shown in figure 3-9. All

the investigations were carried out in the triplicate for reliability and accuracy in the results. The percentage (%) adsorption removal efficiency was calculated using Equation-4. [150]

$$R(\%) = \frac{C_0 - C_t}{C_0} \times 100\ \% \qquad \text{(Eq. 3.4)}$$

Where, is the cadmium removal efficiency, is the initial metal ion (Cd^{+2}) concentration, metal ion (Cd^{+2}) concentration at time t.

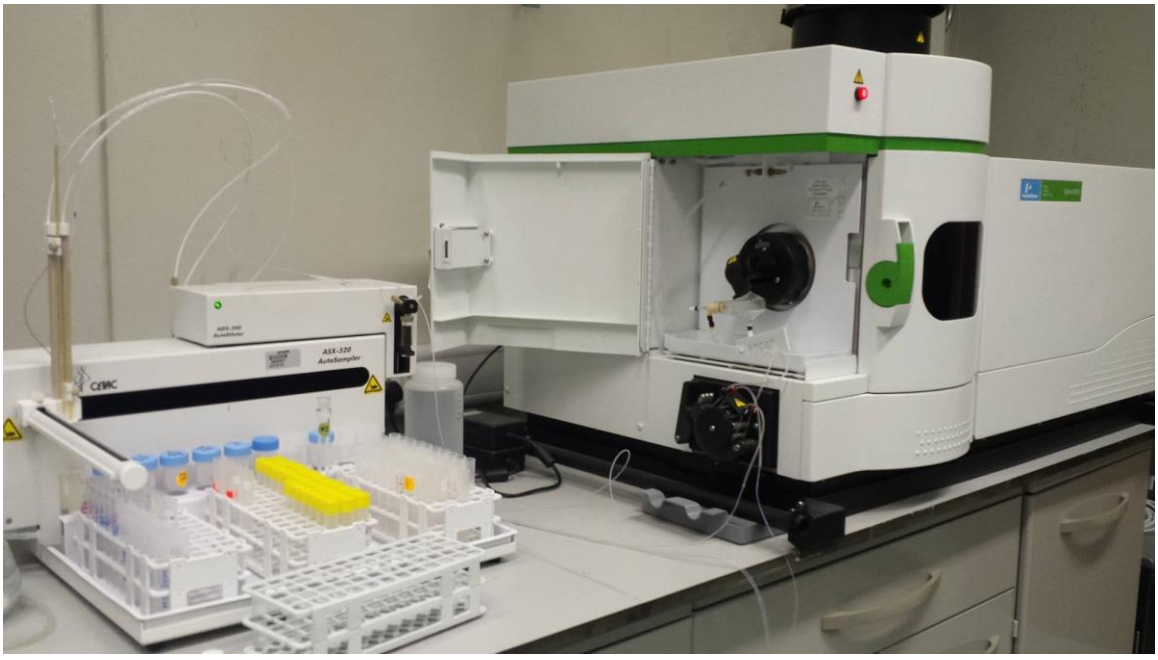

Figure 3-9: Inductively-coupled plasma optical emission spectroscopy (ICP-OES) for Cd concentration test

CHAPTER 4

RESULTS AND DISCUSSION

Pressure-less solid state sintering and spark plasma sintering (SPS) techniques were employed to develop alumina-CNTs nanocomposite membranes. The results were arranged in two separate sections as per the utilized technique.

4.1 Pressure-less Solid State Sintering

An experimental design matrix (shown in table 4-1) was used to evaluate the influence of both applied compaction load on the powder mixture and sintering temperature. The results related to characterization of alumina-CNTs are presented and discussed underneath. The XRD patterns of raw powders (alumina and CNTs) and their nanocomposite mixtures are presented in Fig. 4-1(a). The diffraction peaks of alumina and CNTs matched with the database available in the system PDXL-2. Only alumina peaks appeared in the powder mixture while CNTs peaks didn't show up. There were no additional peaks observed in the sintered samples indicating no new compound or phase formed. Fig. 4-1(b) shows XRD pattern of the four membranes compacted at four different loads and sintered at 1400°C. All the compacted membranes showed the analogous peaks. The FESEM micrographs of as-received alumina (Al_2O_3) and CNTs powders are shown in Fig. 4-2 (a, b).

Table 4-1: Experimental Design (Characteristics of various membranes prepared at different process parameters)

Sample No.	Compaction Load (kN)	Sintering Temperature(°C)	Porosity (%)	Mechanical Strength (MPa)	Average Pore Size (µm)
S1	50	1200	64.6	0.75	0.93
S2	50	1300	61.9	1.74	0.69
S3	50	1400	59.1	2.54	0.55
S4	100	1400	49.5	5.55	0.47
S5	150	1400	45.7	8.43	0.29
S6	200	1400	39.9	11.07	0.15
S7	50	1500	55.4	3.23	0.42
S8	100	1500	46.6	7.87	<0.2
S9	150	1500	40.2	11.91	<0.1
S10	200	1500	31.3	15.64	<0.05

The distribution of carbon nanotubes within the samples was good as SDS and GA were used as CNT dispersants. [147] The CNTs were observed to be located along the grain boundaries and small bundles were also seen inside the big pores, indicating the development of intergranular type nanocomposite. In general, a decreasing trend of the average pore size (~1µm to 0.5 µm) was observed with increasing particle size with sintering temperature that was attributed to the volumetric diffusion of alumina particles. The pore size was calculated by SEM images with the help of image-J software.

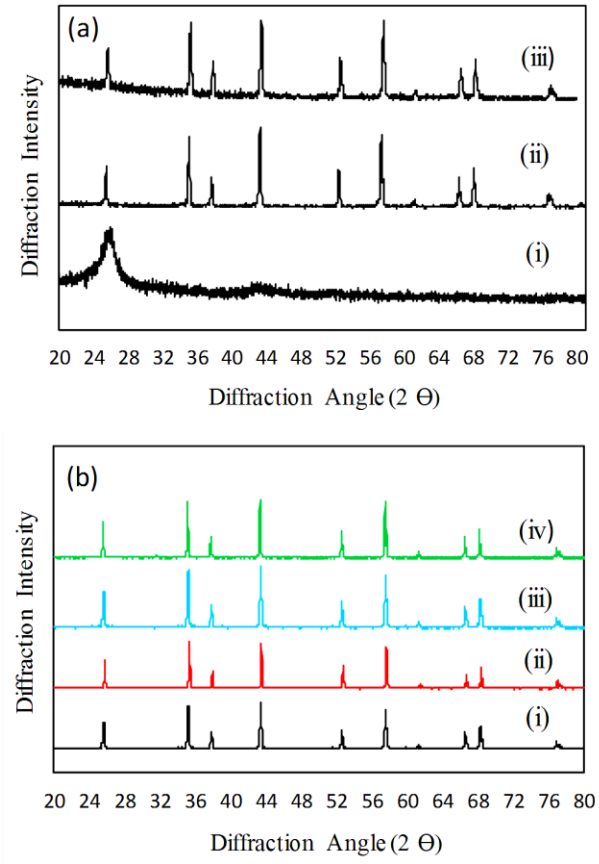

Figure 4-1: (a) XRD pattern (i) CNTs (ii) alumina (iii) powder mixture (alumina-5wt% CNTs) (b): Membranes compacted at (i) 50 kN (ii) 100 kN (iii) 150 kN (iv) 200 kN and sintered at 1400 °C

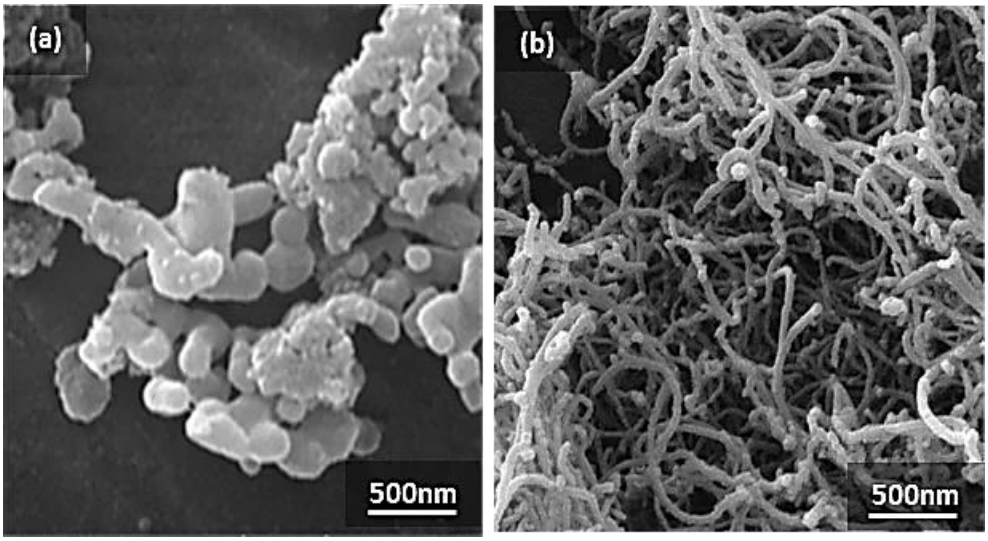

Figure 4-2: FE-SEM micrographs of as-received powders (a) α-alumina (b) raw CNTs

3.4.1 Effect of sintering temperature

The effect of sintering temperature on the overall performance of the membrane was analyzed first. The membrane samples S1, S2, S3, and S7 (Table-4-1) compacted at 50 kN load and sintered at four different temperatures 1200 °C, 1300 °C, 1400 °C and 1500 °C, respectively as shown in Fig. 4-3 (a, b, c, d). Alumina particles growth was observed with increase in sintering temperature. All the samples in Fig. 4-3 depicted large number of pores indicating the successful fabrication of the porous membrane. However, big pores were also observed that were assumed to be formed by the burning of starch (a pore former) during sintering. [44] The samples S1and S2 showed less compressional strengths (0.76 MPa and 1.74 MPa, respectively) because of the high porosities (65% and 62 %). Both samples could not bear pressure above 3 bars during water flux test and fractured. Samples S3 and S7, however, were relatively stronger (2.4, 5.5 MPa) but still had large pores (high porosity and less strength) that made them unsuitable for high flux applications. These samples were also cracked at 5 bar pressure in permeation test.

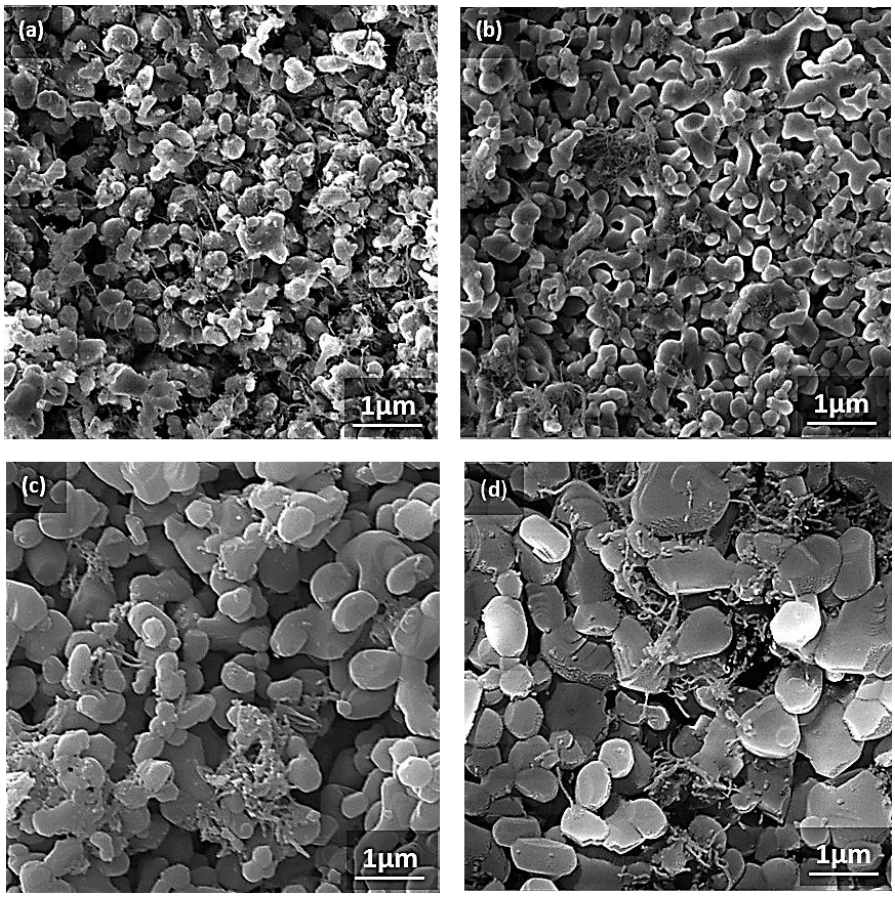

Figure 4-3: Membranes compacted with 50 kN and sintered at (a) 1200 °C (b) 1300 °C (c) 1400 (d) 1500 °C

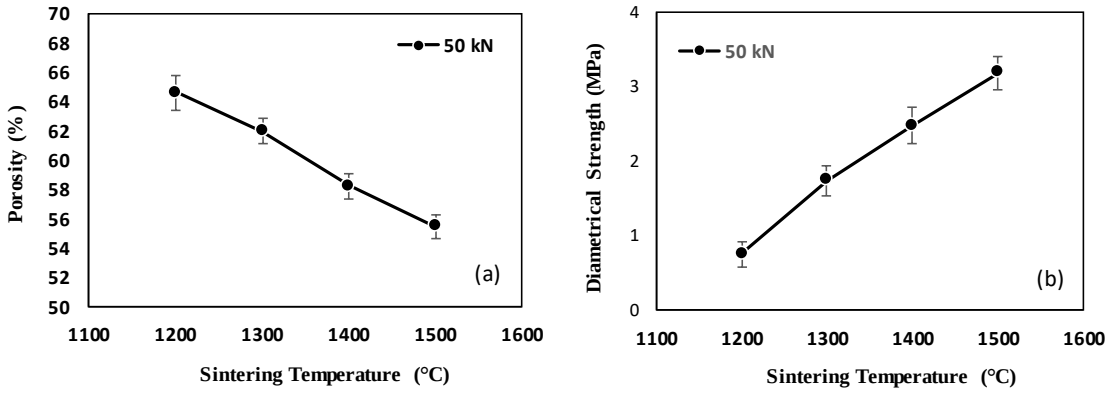

Figure 4-4: : (a) Porosity and (b) strength relationship of the membranes with the change in sintering temperature (compaction load was 50 kN)

3.4.2 Effect of initial compaction load

Higher sintering temperatures (1400°C and 1500°C) were selected, for further study, to analyze alumina-CNTs composite membranes. Now, the initial compaction load of the membranes S4, S5, S6 (sintered at 1400 °C) and S8, S9, and S10 (sintered at 1500 °C) was increased from 50 kN to 100 kN, 150 kN, and 200 kN to obtain higher strengths to make them suitable for high water flux applications. FE-SEM micrographs (Fig. 4-5, 4-6) revealed an increase in the particle size of alumina due to higher grain growth during sintering. The growth was attributed to the coalescence and neck growth of adjacent alumina particles. The higher initial compaction load helped particles to come close to each other during pressing and promote strong network development, as also repeated elsewhere. [23, 32]

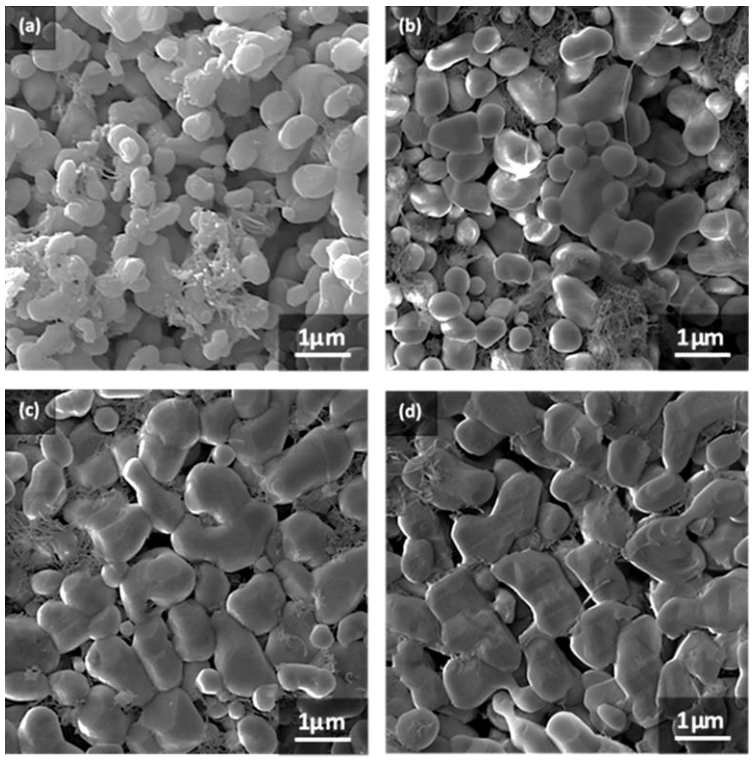

Figure 4-5: FE-SEM images of the membranes compacted at (a) 50 kN (b) 100 kN (c) 150 kN (d) 200 kN loads and sintered at 1400°C

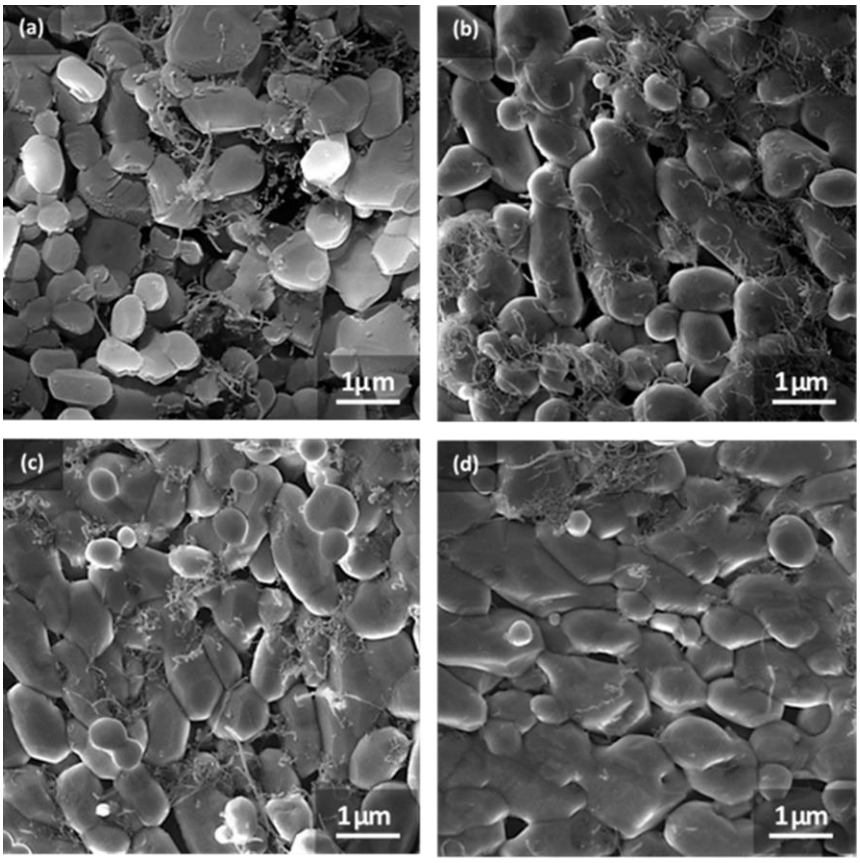

Figure 4-6: FE-SEM images of the membranes compacted at (a) 50 kN (b) 100 kN (c) 150 kN (d) 200 kN loads and sintered at 1500°C

A comparative analysis of measured porosity (through ASTM C373-14a) and strength (through diametrical compression) of these membranes is displayed in Fig. 4-7. A decreasing trend in the porosity of all the samples was observed with increasing compaction load and sintering temperatures, Fig. 4-7(a). Similarly, strength increased with increasing initial compaction loads and sintering temperatures as shown in Fig. 4-7(b). The measured strengths of the present membranes agree with the available literature of diametrical compression test. [12, 48] Interestingly, samples S6 (200 kN/1400°C) and S9 (150 kN/1500°C) showed statistically similar results of porosity (39.9% and 40.2%, respectively) and strengths (11.0 MPa and 11.9 MPa, respectively) as shown with dotted

circle in Fig.4-7. Both samples were also showed similar behavior of water flux as shown in Fig.4-8.

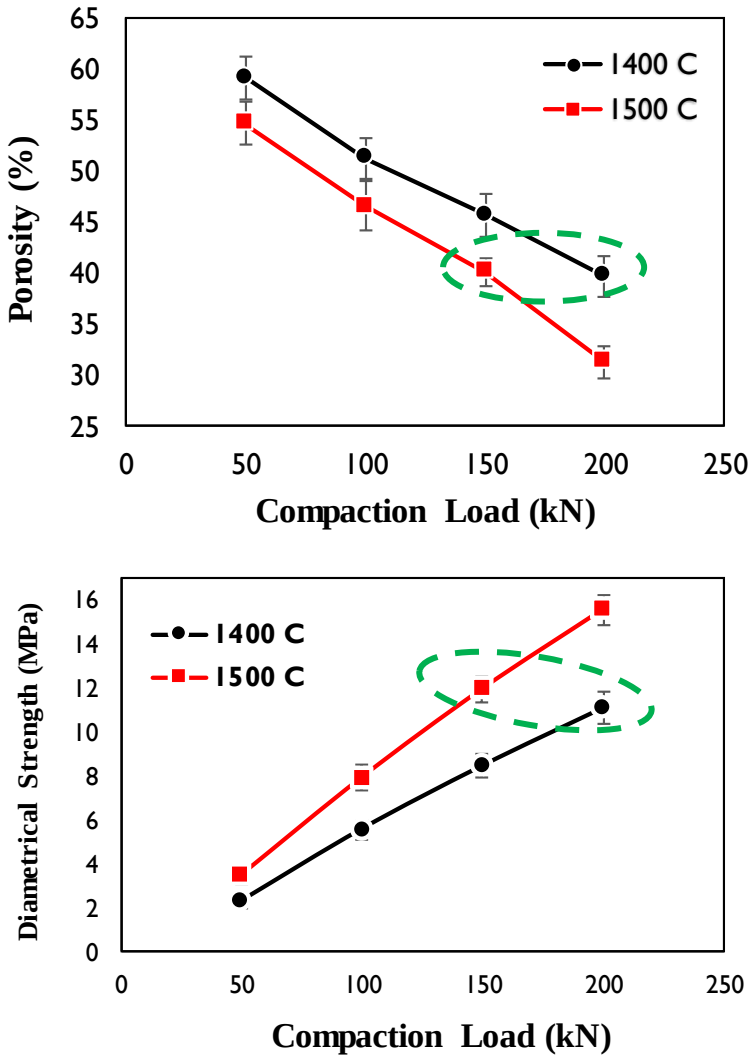

Figure 4-7: (a) Porosity and (b) strength relationship of the membranes with the change in compaction load (sintering temperatures were 1400° C and 1500° C)

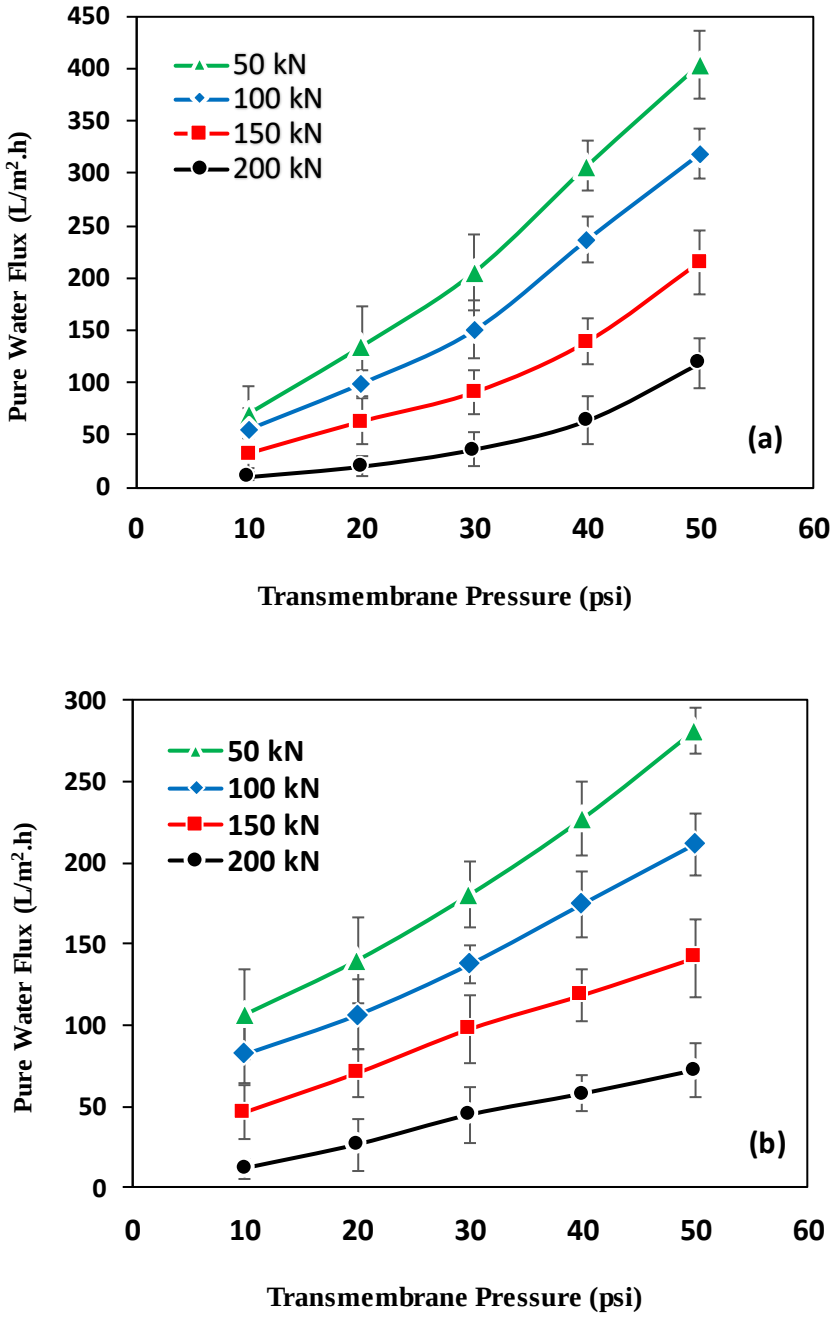

Figure 4-8: Effect of compaction load on water flux sintered at (a) 1400 °C (b) 1500 °C

Water flux values were also influenced by both the process parameters (initial compaction loads and sintering temperatures). Generally, higher flux was investigated in more porous membranes which were compacted with low compaction load and sintered at low temperature. Moreover, a linear increasing trend in water flux was observed in all samples with increasing transmembrane pressure (1 to 5 bar), Fig. 4-8 (a, b). However, sample S10 (200 kN/1500°C) showed least water flux than other samples that might be attributed to the isolations of the pores inside the membranes (pore shrinkage). [151] However, all the membranes developed in the present study, through powder metallurgical route, showed overall higher flux values than CVD method reported to fabricate CNTs-based composite membranes. [54]

4.2 Spark Plasma Sintering (SPS)

An amount of nanocomposite powder was added into a 30-mm graphite die and a graphite sheet was used to facilitate the removal of the sample and to reduce the friction between the die walls and powders. The experiments were conducted in a vacuum with sintering a pressure of (5, 10, 20) MPa, temperature of (1000, 1100, 1200) ^{o}C, heating rate of (50,100,200) ^{o}C/min, and holding time of (2.5, 5, 10) min were used. Parametric study has been conducted to study the effect of SPS parameters on the membrane properties, Table 4-2 shows the different processing parameters sets and the samples code.

Table 4-2: SPS processing parameters, porosity, and diametrical strength

Sample code	T (°C)	t (min)	HR (°C/min)	P (MPa)	Porosity %	diametrical strength (MPa)
1	1000	10	100	20	10.77	12.3
2	1000	10	100	10	56.2	6.9
3	1000	10	100	5.6	69.7	1.9
4	1000	10	50	10	33.2	8
5	1000	10	200	10	60.7	4.9
6	1000	5	200	10	67.5	4.1
7	1000	2.5	200	10	69.3	3.4
11	1100	5	200	10	64	9.5
10N	1200	5	200	10	50	10.4

3.4.3 Characterization of the starting materials

FESEM and XRD were performed for the starting materials to confirm the structure and microstructure. Figure 4-9-a shows the FE-SEM of as received alumina, with a uniform particle size of 0.3 µm which agrees with the supplier data. Moreover, less variation clearly observed from the image which is important to control the pore size. Figure 4-9-b shows FE-SEM micrograph of MWCNTs with an outer diameter (OD) of (10-20 nm). The XRD of CNTs presented in figure 4-10-a shows two peaks corresponding to 2 theta value of 26° and 44° which are related to hexagonal graphite lattice of MWCNT. Figure 4-10-b illustrates the XRD pattern of alumina which shows all the expected peaks of high purity α-alumina.

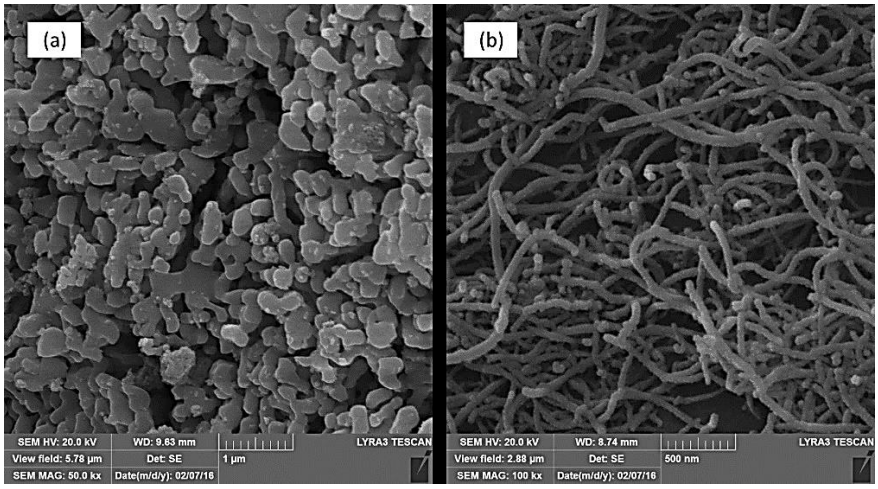

Figure 4-9: FE-SEM image of the as-received materials: (a) α-alumina (b) CNTs

XRD was performed for all the sintered membranes to study the influence of SPS parameters on the structure. Figure 3-c represents the sintered sample at 10 MPa, 1100 ^{o}C, 5 min, 200 C/min. From all the XRD patterns, only the peaks related to crystalline α-Al_2O_3 were observed. The peaks related to the CNTs were not observed because of its small quantity used (5%) as compared to the high crystalline matrix of the alumina. Moreover, in all the XRD pattern, no extra phases or missing peaks were found after sintering which confirmed there were no phase changes occurred during sintering.

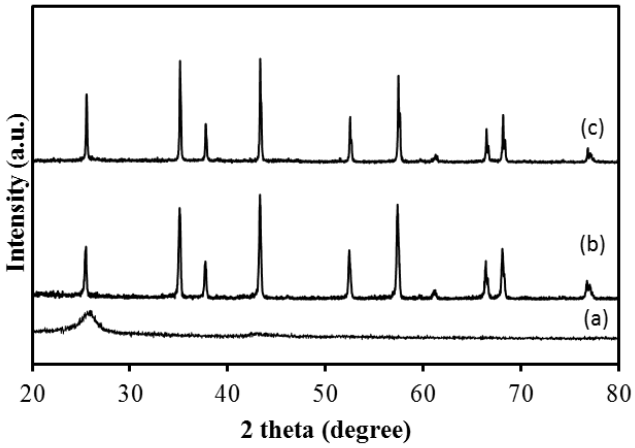

Figure 4-10: XRD patterns of (a) as received CNTs, (b) as received α-alumina, (c) sintered sample at 10 Mpa,1100 oC,5 min, 200 °C/min)

3.4.4 Effect of SPS parameters on porosity, water flux, and permeability

Figure 4-11 depicts the effect of SPS parameters on the porosity and permeability of the SPS samples. The porosity decreased by increasing sintering pressure (figure 4-11a) and temperature (figure 4-11d). However, the porosity has been influenced more by pressure (decreased from 69.7% at 5.5 Mpa to 10.77% at 20 Mpa) compared to the effect of sintering temperature (67% at 1000ºC - 50 % at 1200ºC). Higher temperature and pressure both contributed to neck growth of alumina particle and hence decreased the porosity. The observed decrease in the porosity with increased sintering pressure and temperature might be due to the sintering of the adjacent particles.

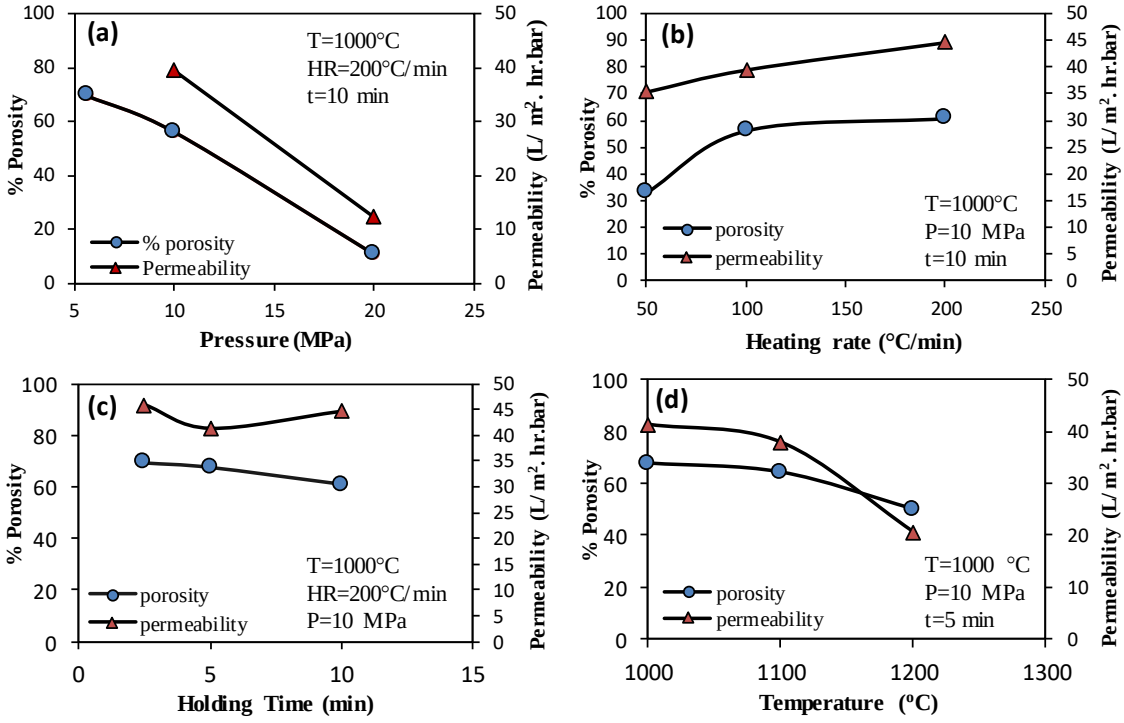

Figure 4-11: Effect of SPS parameters on the porosity and permeability of the membranes: (a) Pressure, (b) Heating rate, (c) Holding time, and (d) Temperature

On the other hand, by increasing heating rate, the porosity was increased (figure 4-11b) (33% at 50 ˚C/min - 69 % at 200 ˚C/min). The opposite effect was observed by the holding time. By increasing the time from 2.5 min to 15 min, the porosity was decreased from 69.3% to 60.7 %(figure 4-11c). The permeability represents the membrane productivity, and it was calculated from the water flux measurements at different sintering conditions as shown in figure 4-12. The permeability has the similar trend of the porosity, decreased by increasing sintering temperature, holding time, and pressure. However, it increased by increasing the heating rate.

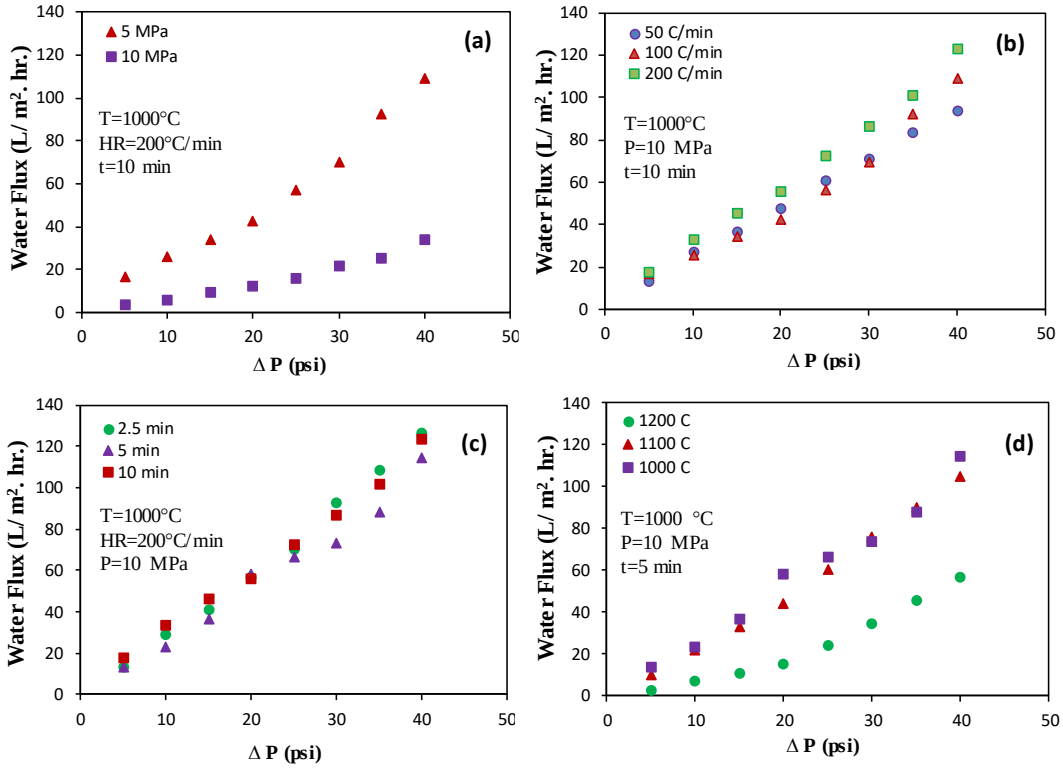

Figure 4-12: Effect of different SPS parameters on pure water flux at different transmittance pressure: (a) Pressure, (b) Heating rate, (c) Holding time, and (d) Temperature

The sample compacted at 5.6 Mpa was broken during the flux test due to the less strength of the membrane at this compacted pressure. The highest permeability was obtained for the samples sintered at 10 Mpa, 1000 ˚C, 2.5 min, 200 ˚C/min, and 10 Mpa, 1000 ˚C, 10 min, 200 ˚C / min. The water flux was measured at a transmembrane pressure of (5-40) psi for the sintered samples using the setup shown in figure 1. The results showed that the water flux increased by increasing the transmittance pressure at all conditions (figure 4-12). The water flux more influenced by SPS pressure (figure 4-12-a) and temperature (figure 4-12-d) which attributed to the percentage of the porosity.

3.4.5 Microstructure characterization of SPS membrane

The FE-SEM was performed for the selected samples to investigate the microstructure and the pore size. Figure 4-13 shows the effect of SPS pressure on the pore size and grain growth. At the sintering pressure of 5.6 MPa (Figure 4-13-a) there was no enough cohesion between particles (fine-grains), however, the size of alumina particles increased due to crystal growth, by increasing the pressure to 10 MPa, and the microstructure becomes denser. The alumina particles have shown neck growth with adjacent particles. This growth increased by increasing sintering pressure (figure 4-13) and sintering temperature (figure 4-14). Figure 4-15 shows a micrograph of the fractured surface of sample 4. It was observed that the CNTs were well distributed within the alumina matrix and located mainly along the grain boundaries. So, the nanocomposite developed in this study seemed to be an intergranular-nanocomposite type [152]. SPS, due to the simultaneous effect of pressure and temperature, enables higher heating rates by shortening the sintering time and temperature as compare to conventional sintering. This helps to obtain fine pores sizes. Therefore, SPS could help to get higher strength at lower temperatures in comparison with

hot pressing [153], and conventional sintering [154]. Figure 8 showed very less porosity and high particle growth at 50 ˚C/min. By decreasing the heating rate, slow sintering occurred which contributed to increase in particle growth and subsequently minimized the numbers of pores. In addition, the grain shape and morphology was also affected. The possible sintering mechanism is believed to be the grain boundary and volumetric diffusion [151], [155]. The average pore size was calculated from all the pores using FE-SEM micrograph for SPS -2 and the average value was 0.201 µm and ranged from 0.05 µm to 0.45 µm. For SPS-11, pore size was 0.143µm ranging from 0.08µm to 0.24 µm. The formation of the pores is attributed to both the burning off the pore former and the partial sintering [156].

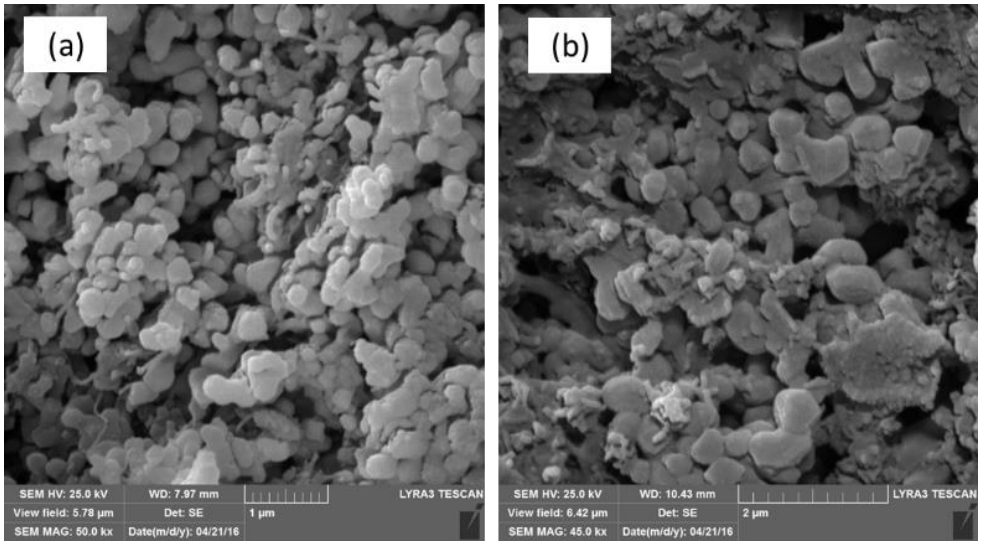

Figure 4-13: FE-SEM of the membrane SPS at different pressure: (a)5.6 MPa,1000 oC,10 min, 100 °C / min, and (b) 10 MPa, 1000 °C,10 min, 100 °C / min

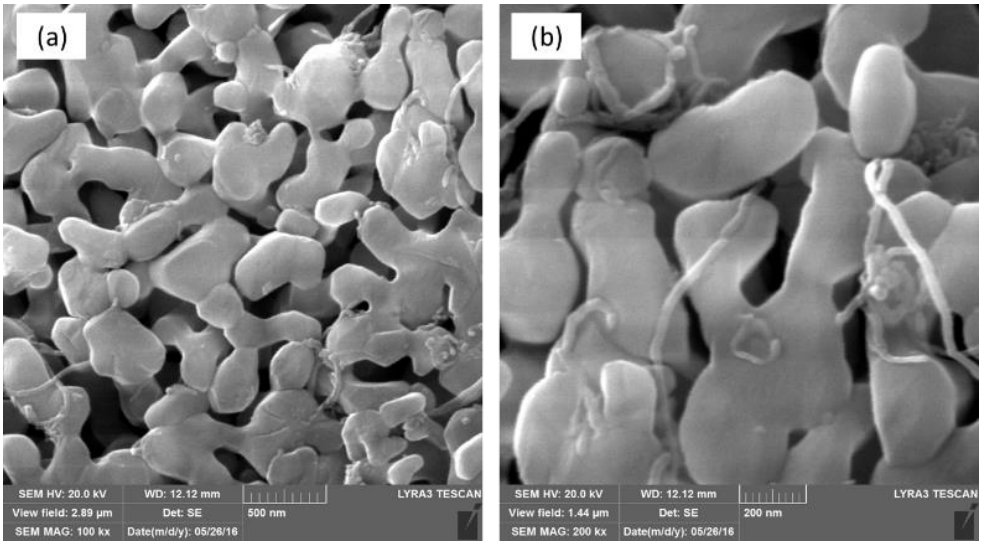

Figure 4-14: FE-SEM of the membrane SPS at 10 MPa, 1100 oC, 5 min, 200 oC/min

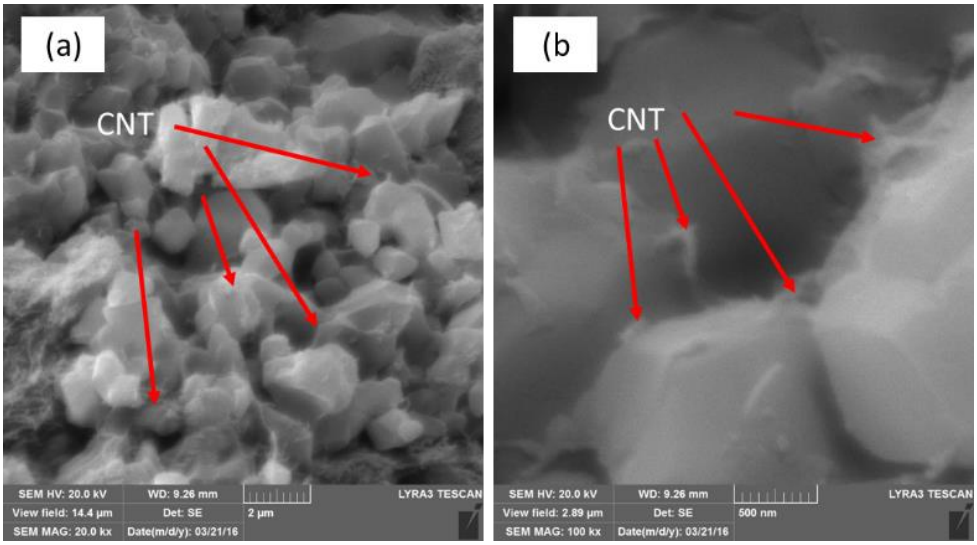

Figure 4-15: FE-SEM micrograph of fracture surfaces of SPS at 10 MPa, 1000 oC,10 min, 50 oC / min

3.4.6 Mechanical properties of alumina-CNTs membrane

The strength of the SPS membrane was increased from 1.9 MPa to 12.3 MPa by increasing the sintering temperature from 1000 ˚C to 1200 ˚C, which was attributed to the growth of the grains and shrinkage of the pores. The same trend of results obtained by increasing

pressure, the sample-1 was sintered with 20 MPa pressure showed 12.3 MPa strength value compared to 1.92 MPa for sample-3 sintered with pressure 5.6 MPa. This revealed that the SPS temperature and pressure have a significant role in the strength of the membrane. High pressure contributes to bringing the particles closer during compaction and high temperature caused them to diffuse in one another easily. The same trend of results obtained [23]. By keeping the other parameters constant, the strength increased by increasing the sintering pressure which was attributed to the increase in the densification of the membrane. The increase in the densification means that increase in the interface formation which ensured effective load sharing between matrix (Al_2O_3) and filler (CNTs), as confirmed by the FE-SEM micrograph shown in figure 4-16. These results agree with the results obtained by [23], [157]. However, the heating rate showed the antagonistic effect on the strength. By increasing the heating rate from 50 ˚C/min to 200 ˚C/min, the strength decreased from 8 Mpa to 4.9 MPa. The reduction in the strength is attributed mainly to the high porosity, a poor interface which remained incapable of proper load sharing. After the diametrical compression test, the sample fractured into two halves (figure 4–16) due to tensile failure [12], which is considered as an indication for successful test [158].

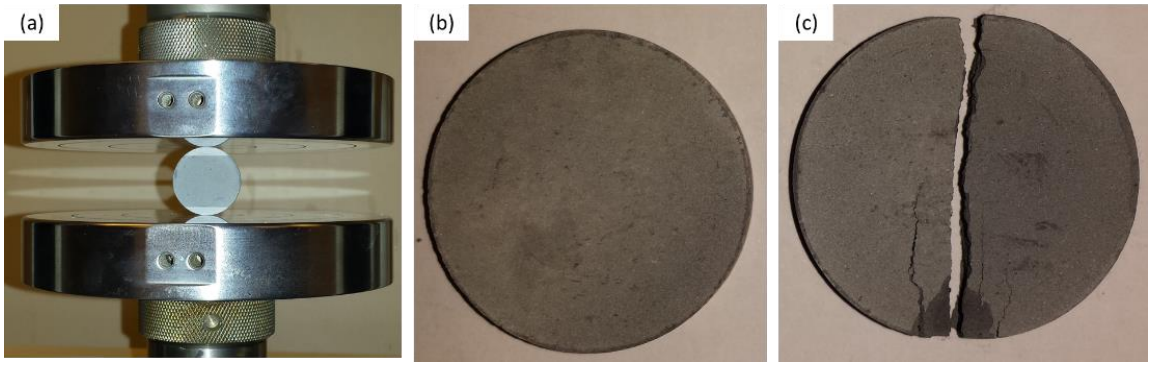

Figure 4-16: Diametrical compression test: (a) configuration, (b) sample before the test, (c) Sample after the test

It is important to analyze and correlate the properties of the developed Al_2O_3-CNTs nanocomposite membranes with the processing parameters to get the best combination of the membrane permeability and strength. The permeability is related to the productivity of the membrane. Moreover, the strength of the membrane has a significant role in the reliability and the operating life of the membrane. The permeability and strength for the membrane at different SPS conditions are presented in figure 4-17 to identify the SPS conditions which give the best combinations between the permeability and strength. The membranes 11 showed the best combinations followed by 2 and 4.

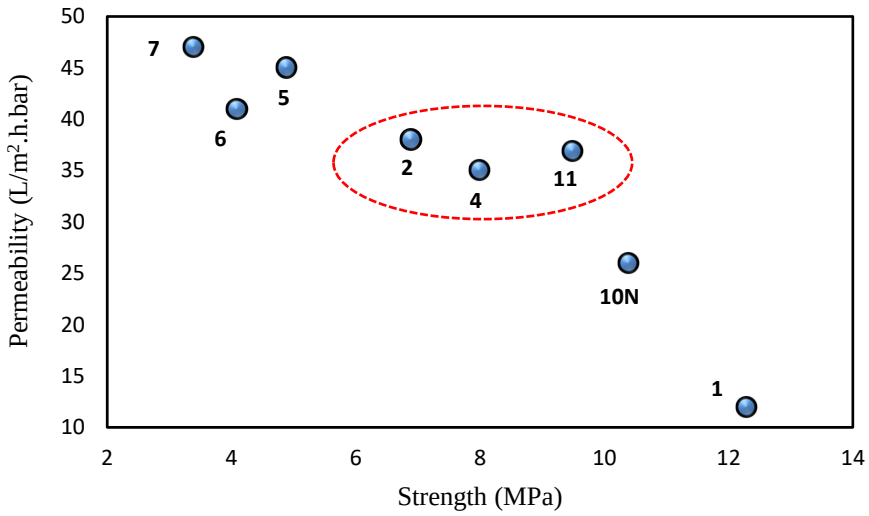

Figure 4-17: permeability and strength of the membrane at different SPS conditions

4.3Removal of cadmium heavy metal from aqueous solution

The solution pH is an important parameter to determine the adsorption mechanism of the heavy metals by the adsorbent material. The cadmium ion (Cd^{+2}) removal experiments were performed using individual alumina and CNTs powders (batch type experiments) in

the pH range 3-8. As shown in Figure 4-18, significant cadmium removal was observed at pH values above 4 for CNTs and above 5 for alumina. Typically, adsorption of cations occurs best at pH closer to neutral and basic medium. In this case, both materials seem to perform best at pH 8, however, when compared with the concentration change in the blank run, Cd cation precipitation could be suspected as a factor [159]. For that, zeta potential analysis was carried out to verify the surface charge of the considered materials. The results shown in Figure 4-19 indicate point of zero charge (pH_{PZC}) to be around pH 5.4 for CNTs and pH 8.3 for alumina. It is known that adsorbent optimum performance occurs at a pH slightly above pH_{PZC} [160].

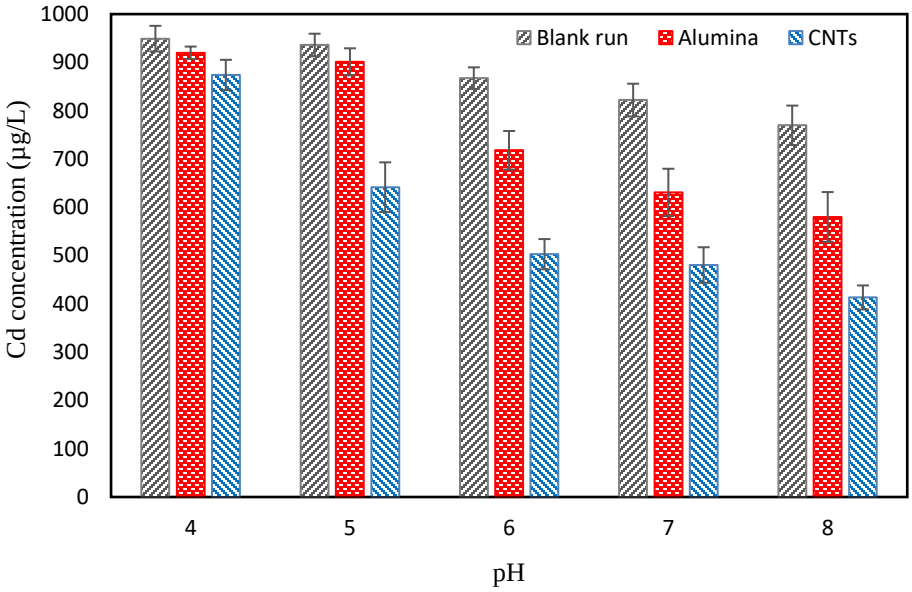

Figure 4-18: Effect of pH on cd+2 removal (Batch experimental runs)

Although, the maximum removal was observed at pH 8, however, the membranes also showed significant removal of Cd at pH 6. As the typical pH of drinking water is in the

range of 6-8, therefore, all the experiments were performed at pH 6 to discover the potential of membranes for the Cd removal for practical applications.

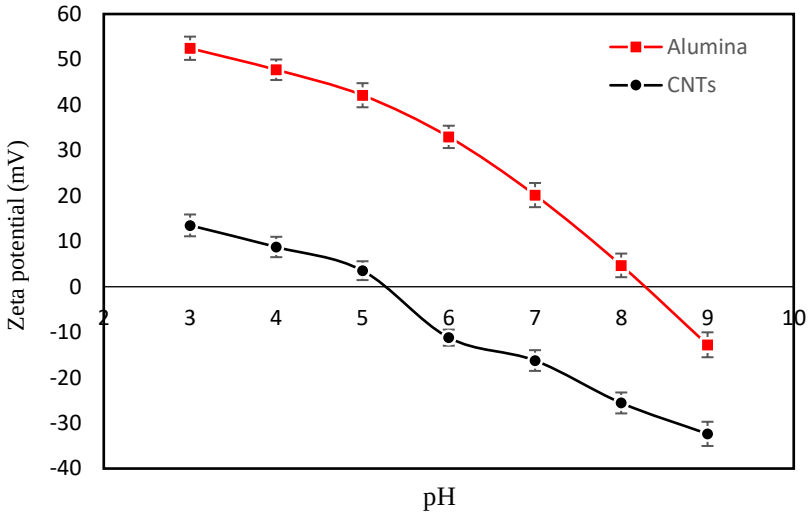

Figure 4-19: Zeta potential analysis of alumina and CNTs powders as a function of pH

After selecting the optimum solution pH, batch adsorption and column tests were carried out to investigate the capacity of alumina-CNT composite in the form of powder mixture and synthesized membrane in removing cadmium from aqueous solution. In the column study, alumina-CNTs membrane, sample S6 (200 kN/1400°C), was installed in the flow loop system and cadmium contaminated water was run through it only once. Fig. 4-20 displays the comparison of the removal efficiency between the alumina-CNTs powder mixture (5wt% CNTs) in batch adsorption and the processed membrane (S6) of the same composition in column study. Although, the material performed well in both situations, an improved rejection of about 93% of cadmium was obtained with the membrane. The improved performance may be attributed to synergistic effect of adsorption and membrane separation (size exclusion).

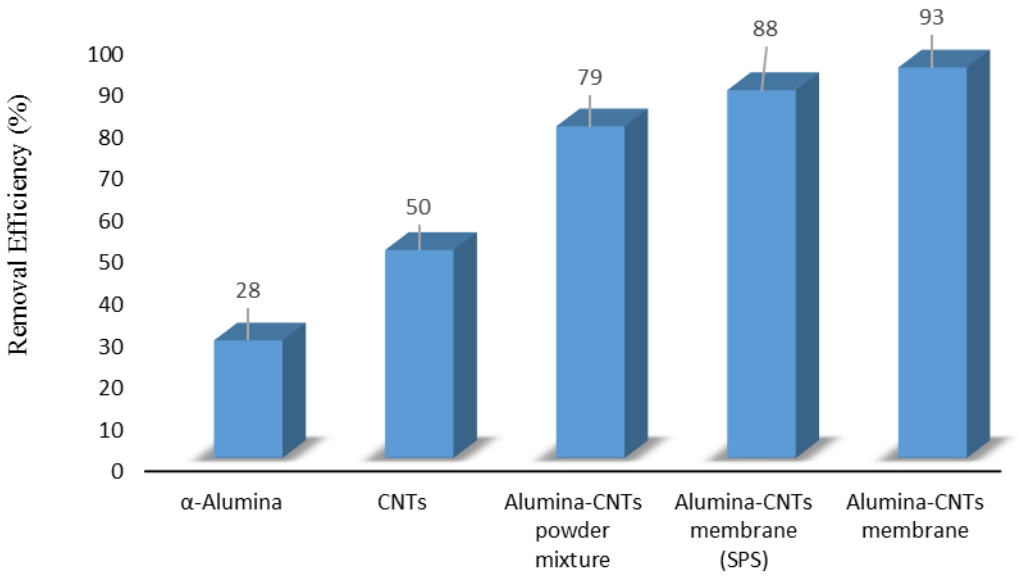

Figure 4-20: Comparison of the removal efficiency of alumina, CNTs, alumina-5wt% CNTs powder mixture and fabricated membrane of same composition

CHAPTER 5

CONCLUSIONS AND RECOMMENDATIONS

5.1 Conclusions

Porous alumina-carbon nanotubes (Al_2O_3-CNTs) nanocomposite membrane fabrication, by conventional pressure-less sintering as well as spark plasma sintering (SPS) techniques, is reported for the first time. The effect of initial compaction load and sintering temperature on the porosity, permeability, water flux, and strength was analyzed. The porosity and strength of the membrane was observed to be influenced by both compaction load and sintering temperature. However, sintering temperature was the primary factor to control pore size and water flux. The best combination of processing parameters was selected by comparing strength with porosity of the membrane. Samples S6 and S9 (compacted at 200 kN and 150 kN loads and sintered at 1400 °C and 1500 °C, respectively) were selected as they showed optimum strength with good permeability. Spark plasma sintering (SPS) technique was also utilized to synthesize Al_2O_3-CNTs nanocomposite membrane. The effect of SPS processing parameters such as pressure, temperature, heating rate, and holding time on the properties of the developed membranes was investigated. The porosity was more influenced by the applied pressure during sintering (decreased from 69.7% at 5.5 MPa to 10.77% at 20 MPa), followed by sintering temperature (69% at 1000 ˚C - 50 % at 1200 ˚C). The strength, water flux, and permeability of the membrane were also affected by the sintering temperature and pressure consequently. Zeta-potential analysis and batch

adsorption experimentations helped to select pH 6 for cadmium removal tests. Finally, the cadmium (Cd^{+2}) ion removal efficiency of the alumina, CNTs, their powder mixture (5wt %CNTs) through batch adsorption experimentations and that of the developed membrane, using the flow loop system, was analyzed. The highest (93%) of Cd+2 removal was obtained from pressure-less sintered membrane (200kN/1400°C), through physical adsorption, from water containing 1ppm cadmium solution at pH 6.

5.2 Recommendations

The following aspects can be addressed in the future work:

1. Removal efficiency of the developed membranes of other heavy metal ions such as arsenic (As^{+2}), mercury (Hg^{+2}), and lead (Pb^{+2}).
2. Effect of carbon nanotubes (CNTs) loading, in the composite membrane, on the porosity, strength, and heavy metal removal efficiency.
3. Surface modifications of the CNTs (impregnated of chemically functionalized/ oxidized) on the adsorption capacity of the membrane.
4. Use of other type of alumina such as activated alumina, nano alumina (≤ 100 nm), and gamma-alumina.

References

[1] WHO and Unicef, "Progress on Drinking Water and Sanitation-2014 Update," *Jt. Monit. Program. Water Supply Sanit.*, pp. 1–78, 2014.

[2] X. Qu, P. J. J. Alvarez, and Q. Li, "Applications of nanotechnology in water and wastewater treatment," *Water Res.*, vol. 47, no. 12, pp. 3931–3946, 2013.

[3] M. N. and L. T. F. Gunnar F. Nordberg, Bruce A. Fowler, *Handbook on the Toxicology of Metals (Third Edition)*. .

[4] D. Mohan and C. U. Pittman, "Arsenic removal from water/wastewater using adsorbents-A critical review," *J. Hazard. Mater.*, vol. 142, no. 1–2, pp. 1–53, 2007.

[5] G. Zhao, X. Wu, X. Tan, and X. Wang, "Sorption of Heavy Metal Ions from Aqueous Solutions: A Review," *Open Colloid Sci. J.*, vol. 4, no. Ii, pp. 19–31, 2011.

[6] F. Fu and Q. Wang, "Removal of heavy metal ions from wastewaters: A review," *J. Environ. Manage.*, vol. 92, no. 3, pp. 407–418, 2011.

[7] Ihsanullah *et al.*, "Heavy metal removal from aqueous solution by advanced carbon nanotubes: Critical review of adsorption applications," *Sep. Purif. Technol.*, vol. 157, no. January, pp. 141–161, 2016.

[8] B. Van Der Bruggen, C. Vandecasteele, T. Van Gestel, W. Doyen, and R. Leysen, "A review of pressure-driven membrane processes in wastewater treatment and drinking water production," *Environ. Prog.*, vol. 22, no. 1, pp. 46–56, 2003.

[9] G. P. Rao, C. Lu, and F. Su, "Sorption of divalent metal ions from aqueous solution by carbon nanotubes: A review," *Sep. Purif. Technol.*, vol. 58, no. 1, pp. 224–231, 2007.

[10] T. S. Y. Choong, T. G. Chuah, Y. Robiah, F. L. Gregory Koay, and I. Azni, "Arsenic toxicity, health hazards and removal techniques from water: an overview," *Desalination*, vol. 217, no. 1–3, pp. 139–166, 2007.

[11] X. Bernat *et al.*, "Non-enhanced ultrafiltration of iron(III) with commercial ceramic membranes," *J. Memb. Sci.*, vol. 334, no. 1–2, pp. 129–137, 2009.

[12] F. Patel, M. A. Baig, and T. Laoui, "Processing of porous alumina substrate for multilayered ceramic filter," *Desalin. Water Treat.*, vol. 35, no. 1–3, pp. 33–38, 2011.

[13] T. Ebadzadeh, A. Behnamghader, and R. Nemati, "Preparation of porous hydroxyapatite ceramics containing mullite by reaction sintering of clay, alumina and hydroxyapatite," *Ceram. Int.*, vol. 37, no. 7, pp. 2887–2889, 2011.

[14] J. Kim and B. Van Der Bruggen, "The use of nanoparticles in polymeric and ceramic membrane structures: Review of manufacturing procedures and performance improvement for water treatment," *Environ. Pollut.*, vol. 158, no. 7, pp. 2335–2349, 2010.

[15] V. Zaspalis, A. Pagana, and S. Sklari, "Arsenic removal from contaminated water by iron oxide sorbents and porous ceramic membranes," *Desalination*, vol. 217, no. 1–3, pp. 167–180, 2007.

[16] R. Allabashi, M. Arkas, G. Hörmann, and D. Tsiourvas, "Removal of some organic pollutants in water employing ceramic membranes impregnated with cross-linked silylated dendritic and cyclodextrin polymers," *Water Res.*, vol. 41, no. 2, pp. 476–

486, 2007.
[17] A. Alpatova, E. S. Kim, S. Dong, N. Sun, P. Chelme-Ayala, and M. Gamal El-Din, “Treatment of oil sands process-affected water with ceramic ultrafiltration membrane: Effects of operating conditions on membrane performance,” *Sep. Purif. Technol.*, vol. 122, pp. 170–182, 2014.
[18] M. Ebrahimi *et al.*, “Investigations on the use of different ceramic membranes for efficient oil-field produced water treatment,” *Desalination*, vol. 250, no. 3, pp. 991–996, 2010.
[19] R. K. Ahluwalia, K. H. Im, H. K. Geyer, D. L. Shelleman, and R. E. Tressler, “Performance of Ceramic Membrane Filters.”
[20] P. Biesheuvel and H. Verweij, “Design of ceramic membrane supports: permeability, tensile strength and stress,” *J. Memb. Sci.*, 1999.
[21] M. Fukushima, Y. Zhou, and H. Miyazaki, “Microstructural characterization of porous silicon carbide membrane support with and without alumina additive,” *J.*, 2006.
[22] A. Chinelatto and R. Tomasi, “Influence of processing atmosphere on the microstructural evolution of submicron alumina powder during sintering,” *Ceram. Int.*, 2009.
[23] S. Barma and B. Mandal, “Effects of sintering temperature and initial compaction load on alpha-alumina membrane support quality,” *Ceram. Int.*, vol. 40, no. 7 PART B, pp. 11299–11309, 2014.
[24] D. Jayaseelan, N. Kondo, and M. Brito, “High-Strength Porous Alumina Ceramics by the Pulse Electric Current Sintering Technique,” *J. Am.*, 2002.
[25] F. Patel, M. Baig, and T. Laoui, “Processing of porous alumina substrate for multilayered ceramic filter,” *Desalin. Water Treat.*, 2011.
[26] B. Nandi, R. Uppaluri, and M. Purkait, “Preparation and characterization of low cost ceramic membranes for micro-filtration applications,” *Appl. Clay Sci.*, 2008.
[27] C. Falamaki, M. Afarani, and A. Aghaie, “Initial sintering stage pore growth mechanism applied to the manufacture of ceramic membrane supports,” *J. Eur. Ceram.*, 2004.
[28] Y. Wang, T. Tian, X. Liu, and G. Meng, “Titania membrane preparation with chemical stability for very hash environments applications,” *J. Memb. Sci.*, 2006.
[29] Y. Yoshino, T. Suzuki, B. Nair, and H. Taguchi, “Development of tubular substrates, silica based membranes and membrane modules for hydrogen separation at high temperature,” *J. Membr.*, 2005.
[30] N. Saffaj, S. Younssi, A. Albizane, and A. Messouadi, “Preparation and characterization of ultrafiltration membranes for toxic removal from wastewater,” *Desalination*, 2004.
[31] W. Qin, C. Peng, M. Lv, and J. Wu, “Preparation and properties of high-purity porous alumina support at low sintering temperature,” *Ceram. Int.*, 2014.
[32] K. Shafiei, M. Kazemimoghaddam, T. Mohammadi, and S. Ghanbari Pakdehi, “An investigation on manufacturing of alumina microfiltration membranes,” *Desalin. Water Treat.*, vol. 867539, no. January 2014, pp. 1–9, 2013.
[33] K. H. Kim, S. J. Cho, K. J. Yoon, J. J. Kim, J. Ha, and D. I. I. Chun, “Centrifugal casting of alumina tube for membrane application,” *J. Memb. Sci.*, vol. 199, no. 1, pp. 69–74, 2002.

[34] G. C. Steenkamp, H. W. J. P. Neomagus, H. M. Krieg, and K. Keizer, “Centrifugal casting of ceramic membrane tubes and the coating with chitosan,” *Sep. Purif. Technol.*, vol. 25, no. 1–3, pp. 407–413, 2001.
[35] M. Cervera, M. Arnal, and M. de la Guardia, “Removal of heavy metals by using adsorption on alumina or chitosan,” *Anal. Bioanal.*, 2003.
[36] L. Zhang, T. Huang, M. Zhang, X. Guo, and Z. Yuan, “Studies on the capability and behavior of adsorption of thallium on nano-Al 2 O 3,” *J. Hazard.*, 2008.
[37] M. Revathi, B. Kavitha, and T. Vasudevan, “Removal of nickel ions from industrial plating effluents using activated alumina as adsorbent.,” *J. Environ.*, 2005.
[38] M. J. Santos Yabe and E. de Oliveira, “Heavy metals removal in industrial effluents by sequential adsorbent treatment,” *Adv. Environ. Res.*, vol. 7, no. 2, pp. 263–272, 2003.
[39] M. M. Pendergast and E. M. V Hoek, “A review of water treatment membrane nanotechnologies.”
[40] K.-J. Lee and H.-D. Park, “Effect of transmembrane pressure, linear velocity, and temperature on permeate water flux of high-density vertically aligned carbon nanotube membranes,” *Desalin. Water Treat.*, vol. 57, no. 55, pp. 26706–26717, Nov. 2016.
[41] K. Goh *et al.*, “Carbon nanomaterials for advancing separation membranes: A strategic perspective,” *Carbon N. Y.*, vol. 109, pp. 694–710, 2016.
[42] R. Das, M. E. Ali, S. B. A. Hamid, S. Ramakrishna, and Z. Z. Chowdhury, “Carbon nanotube membranes for water purification: A bright future in water desalination,” *Desalination*, vol. 336, pp. 97–109, 2014.
[43] J. Kim and B. Van der Bruggen, “The use of nanoparticles in polymeric and ceramic membrane structures: Review of manufacturing procedures and performance improvement for water treatment,” *Environ. Pollut.*, vol. 158, no. 7, pp. 2335–2349, 2010.
[44] M. F. L. De Volder, S. H. Tawfick, R. H. Baughman, and A. J. Hart, “Carbon Nanotubes: Present and Future Commercial Applications,” *Science (80-.).*, vol. 339, no. 6119, 2013.
[45] T. Altalhi, M. Ginic-Markovic, N. Han, S. Clarke, and D. Losic, “Synthesis of carbon nanotube (CNT) composite membranes,” *Membranes (Basel).*, vol. 1, no. 1, pp. 37–47, 2010.
[46] H. Parham, A. Kennedy, and Y. Zhu, “Preparation of porous alumina–carbon nanotube composites via direct growth of carbon nanotubes,” *Compos. Sci. Technol.*, vol. 71, no. 15, pp. 1739–1745, 2011.
[47] H. Parham, S. Bates, Y. Xia, and Y. Zhu, “A highly efficient and versatile carbon nanotube/ceramic composite filter,” *Carbon N. Y.*, vol. 54, pp. 215–223, 2013.
[48] Ihsanullah *et al.*, “Novel anti-microbial membrane for desalination pretreatment: A silver nanoparticle-doped carbon nanotube membrane,” *Desalination*, vol. 376, pp. 82–93, 2015.
[49] T. Ostrowski and J. Rödel, “Evolution of mechanical properties of porous alumina during free sintering and hot pressing,” *J. Am. Ceram. Soc.*, 1999.
[50] Z. Deng, T. Fukasawa, and M. Ando, “Microstructure and mechanical properties of porous alumina ceramics fabricated by the decomposition of aluminum hydroxide,” *J.*, 2001.

[51] D. Jayaseelan, N. Kondo, and M. Brito, “High-Strength Porous Alumina Ceramics by the Pulse Electric Current Sintering Technique,” *J. Am.*, 2002.
[52] S.-T. Oh, K. Tajima, M. Ando, and T. Ohji, “Strengthening of Porous Alumina by Pulse Electric Current Sintering and Nanocomposite Processing,” *J. Am. Ceram. Soc.*, vol. 83, no. 5, pp. 1314–1316, Dec. 2004.
[53] D. Green, C. Nader, and R. Brezny, “Elastic behaviour of partially-sintered alumina,” *Proc. Symp. Sinter. Adv. Ceram. …*, 1988.
[54] D. Lam, F. Lange, and A. Evans, “Mechanical properties of partially dense alumina produced from powder compacts,” *J. Am.*, 1994.
[55] S. Nanjangud and R. Brezny, “Strength and Young’s modulus behavior of a partially sintered porous alumina,” *J. Am.*, 1995.
[56] C. Kawai and A. Yamakawa, “Effect of porosity and microstructure on the strength of Si3N4: designed microstructure for high strength, high thermal shock resistance, and facile machining,” *J. Am. Ceram.*, 1997.
[57] G. Li, Z. Jiang, A. Jiang, and L. Zhang, “Strengthening of porous Al2O3 ceramics through nanoparticle addition,” *Nanostructured Mater.*, 1997.
[58] M. Mahmoud, A. El-Latif, A. M. Ibrahim, M. S. Showman, and R. R. A. Hamide, “Alumina/Iron Oxide Nano Composite for Cadmium Ions Removal from Aqueous Solutions,” *Int. J. Nonferrous Metall.*, vol. 2, pp. 47–62, 2013.
[59] G. Nordberg, *Handbook on the toxicology of metals*. Academic Press, 2007.
[60] J. Wang and C. Chen, “Biosorbents for heavy metals removal and their future,” *Biotechnol. Adv.*, vol. 27, no. 2, pp. 195–226, 2009.
[61] J. Wang and C. Chen, “Biosorption of heavy metals by Saccharomyces cerevisiae: A review,” *Biotechnol. Adv.*, vol. 24, no. 5, pp. 427–451, Sep. 2006.
[62] R. Singh, N. Gautam, A. Mishra, and R. Gupta, “Heavy metals and living systems: An overview.,” *Indian J. Pharmacol.*, vol. 43, no. 3, pp. 246–53, May 2011.
[63] A.-F. Ngomsik, A. Bee, J.-M. Siaugue, D. Talbot, V. Cabuil, and G. Cote, “Co(II) removal by magnetic alginate beads containing Cyanex 272.,” *J. Hazard. Mater.*, vol. 166, no. 2–3, pp. 1043–9, Jul. 2009.
[64] S. K. R. Yadanaparthi, D. Graybill, and R. von Wandruszka, “Adsorbents for the removal of arsenic, cadmium, and lead from contaminated waters,” *J. Hazard. Mater.*, vol. 171, no. 1–3, pp. 1–15, Nov. 2009.
[65] B. Volesky, “Detoxification of metal-bearing effluents: biosorption for the next century,” *Hydrometallurgy*, vol. 59, no. 2, pp. 203–216, 2001.
[66] A. Afkhami, T. Madrakian, A. Amini, and Z. Karimi, “Effect of the impregnation of carbon cloth with ethylenediaminetetraacetic acid on its adsorption capacity for the adsorption of several metal ions,” *J. Hazard. Mater.*, vol. 150, no. 2, pp. 408–412, 2008.
[67] F. Fu and Q. Wang, “Removal of heavy metal ions from wastewaters: A review,” *J. Environ. Manage.*, vol. 92, no. 3, pp. 407–418, 2011.
[68] J. M. Dias, M. C. M. Alvim-Ferraz, M. F. Almeida, J. Rivera-Utrilla, and M. Sánchez-Polo, “Waste materials for activated carbon preparation and its use in aqueous-phase treatment: A review,” *J. Environ. Manage.*, vol. 85, no. 4, pp. 833–846, 2007.
[69] A. Jusoh, L. Su Shiung, N. Ali, and M. J. M. M. Noor, “A simulation study of the removal efficiency of granular activated carbon on cadmium and lead,”

Desalination, vol. 206, no. 1–3, pp. 9–16, Feb. 2007.
[70] K. Kang, S. Kim, J. Choi, and S. Kwon, "Sorption of Cu 2+ and Cd 2+ onto acid- and base-pretreated granular activated carbon and activated carbon fiber samples," *Eng. Chem.*, 2008.
[71] M. Rao, D. Ramana, K. Seshaiah, and M. Wang, "Removal of some metal ions by activated carbon prepared from Phaseolus aureus hulls," *J. Hazard.*, 2009.
[72] V. K. Gupta, M. Gupta, and S. Sharma, "Process development for the removal of lead and chromium from aqueous solutions using red mud—an aluminium industry waste," *Water Res.*, vol. 35, no. 5, pp. 1125–1134, 2001.
[73] M. A. Barakat, "New trends in removing heavy metals from industrial wastewater," *Arab. J. Chem.*, vol. 4, no. 4, pp. 361–377, 2011.
[74] K. Ishizaki and M. Nanko, "A hot isostatic process for fabricating porous materials," *J. Porous Mater.*, vol. 1, no. 1, pp. 19–27, 1995.
[75] Y. C. Sharma, V. Srivastava, S. N. Upadhyay, and C. H. Weng, "Alumina Nanoparticles for the Removal of Ni(II) from Aqueous Solutions," *Ind. Eng. Chem. Res.*, vol. 47, no. 21, pp. 8095–8100, Nov. 2008.
[76] L. Zhang, T. Huang, M. Zhang, X. Guo, and Z. Yuan, "Studies on the capability and behavior of adsorption of thallium on nano-Al2O3," *J. Hazard. Mater.*, vol. 157, no. 2, pp. 352–357, 2008.
[77] A. R. Türker, "New Sorbents for Solid-Phase Extraction for Metal Enrichment," *CLEAN – Soil, Air, Water*, vol. 35, no. 6, pp. 548–557, Dec. 2007.
[78] D. Yang *et al.*, "Alumina nanofibers grafted with functional groups: A new design in efficient sorbents for removal of toxic contaminants from water," *Water Res.*, vol. 44, no. 3, pp. 741–750, 2010.
[79] M. Luisa Cervera, M. Carmen Arnal, and M. de la Guardia, "Removal of heavy metals by using adsorption on alumina or chitosan," *Anal. Bioanal. Chem.*, vol. 375, no. 6, pp. 820–825, Mar. 2003.
[80] †,‡ L. Ji, † J. Lin, † and K. L. Tan, and ‡ H. C. Zeng*, "Synthesis of High-Surface-Area Alumina Using Aluminum Tri-sec-butoxide−2,4-Pentanedione− 2-Propanol−Nitric Acid Precursors," 2000.
[81] I. Nettleship, "Applications of Porous Ceramics," *Key Eng. Mater.*, vol. 122–124, pp. 305–324, 1996.
[82] G. R. Doughty and D. Hind, "The Applications of Ion-Conducting Ceramics," *Key Eng. Mater.*, vol. 122–124, pp. 145–162, 1996.
[83] K. J. Farley, D. A. Dzombak, and F. M. . Morel, "A surface precipitation model for the sorption of cations on metal oxides," *J. Colloid Interface Sci.*, vol. 106, no. 1, pp. 226–242, Jul. 1985.
[84] M. Anderson and A. Rubin, "Adsorption of inorganics at solid-liquid interfaces," 1981.
[85] P. Schindler, W. Stumm, and W. Stumm, "Aquatic surface chemistry," *Ed. by W. Stumm*, 1987.
[86] C. Tiffreau, J. Lützenkirchen, and P. Behra, "Modeling the adsorption of mercury (II) on (hydr) oxides: I. Amorphous iron oxide and α-quartz," *J. Colloid Interface*, 1995.
[87] L. Gunneriusson, "Composition and stability of Cd (II)-chloro and-hydroxo complexes at the goethite (α-FeOOH)/water interface," *J. Colloid Interface Sci.*,

1994.
[88] M. Kosmulski, “Adsorption of cadmium on alumina and silica: analysis of the values of stability constants of surface complexes calculated for different parameters of triple layer model,” *Colloids Surfaces A Physicochem. Eng. Asp.*, vol. 117, no. 3, pp. 201–214, Oct. 1996.
[89] J. Liu, Z. Zhao, and G. Jiang, “Coating Fe 3 O 4 Magnetic Nanoparticles with Humic Acid for High Efficient Removal of Heavy Metals in Water,” *Environ. Sci. Technol.*, vol. 42, no. 18, pp. 6949–6954, Sep. 2008.
[90] A.-F. Ngomsik, A. Bee, M. Draye, G. Cote, and V. Cabuil, “Magnetic nano- and microparticles for metal removal and environmental applications: a review,” *Comptes Rendus Chim.*, vol. 8, no. 6, pp. 963–970, 2005.
[91] D. Yang *et al.*, “Layered Titanate Nanofibers as Efficient Adsorbents for Removal of Toxic Radioactive and Heavy Metal Ions from Water,” *J. Phys. Chem. C*, vol. 112, no. 42, pp. 16275–16280, Oct. 2008.
[92] N. Savage and M. S. Diallo, “Nanomaterials and Water Purification: Opportunities and Challenges,” *J. Nanoparticle Res.*, vol. 7, no. 4–5, pp. 331–342, Oct. 2005.
[93] X. Ren, C. Chen, M. Nagatsu, and X. Wang, “Carbon nanotubes as adsorbents in environmental pollution management: A review,” *Chem. Eng. J.*, vol. 170, no. 2, pp. 395–410, 2011.
[94] “Helical Microtubules of Graphitic Carbon.”
[95] *,† Sandeep Agnihotri, *,‡ José P. B. Mota, § and Massoud Rostam-Abadi, and M. J. Rood⊥, “Theoretical and Experimental Investigation of Morphology and Temperature Effects on Adsorption of Organic Vapors in Single-Walled Carbon Nanotubes,” 2006.
[96] M. Muris, N. Dupont-Pavlovsky, M. Bienfait, and P. Zeppenfeld, “Where are the molecules adsorbed on single-walled nanotubes?,” *Surf. Sci.*, vol. 492, no. 1, pp. 67–74, 2001.
[97] S. M. Gatica, M. J. Bojan, G. Stan, and M. W. Cole, “Quasi-one- and two-dimensional transitions of gases adsorbed on nanotube bundles,” *J. Chem. Phys.*, vol. 114, no. 8, pp. 3765–3769, Feb. 2001.
[98] O. Byl *et al.*, “Adsorption of CF 4 on the Internal and External Surfaces of Opened Single-Walled Carbon Nanotubes: A Vibrational Spectroscopy Study.”
[99] † Sandeep Agnihotri, *,‡ José P. B. Mota, *,†,§ and Massoud Rostam-Abadi, and M. J. Rood†, “Structural Characterization of Single-Walled Carbon Nanotube Bundles by Experiment and Molecular Simulation,” 2005.
[100] M. R. Babaa, I. Stepanek, K. Masenelli-Varlot, N. Dupont-Pavlovsky, E. McRae, and P. Bernier, “Opening of single-walled carbon nanotubes: evidence given by krypton and xenon adsorption,” *Surf. Sci.*, vol. 531, no. 1, pp. 86–92, 2003.
[101] M. L. Toebes, J. M. . van Heeswijk, J. H. Bitter, A. Jos van Dillen, and K. P. de Jong, “The influence of oxidation on the texture and the number of oxygen-containing surface groups of carbon nanofibers,” *Carbon N. Y.*, vol. 42, no. 2, pp. 307–315, 2004.
[102] J. Liu *et al.*, “Fullerene Pipes,” *Science (80-.).*, vol. 280, no. 5367, 1998.
[103] O. Byl, J. Liu, and J. T. Yates, “Etching of Carbon Nanotubes by OzoneA Surface Area Study Etching of Carbon Nanotubes by OzonesA Surface Area Study,” *Langmuir*, vol. 21, no. 9, pp. 4200–4204, 2005.

[104] L. Vincent Liu, W. Quan Tian, and Y. Alexander Wang, “Ozonization at the Vacancy Defect Site of the Single-Walled Carbon Nanotube.”
[105] M.-L. Sham and J.-K. Kim, “Surface functionalities of multi-wall carbon nanotubes after UV/Ozone and TETA treatments,” *Carbon N. Y.*, vol. 44, no. 4, pp. 768–777, 2006.
[106] C. Chen, B. Liang, A. Ogino, X. Wang, and M. Nagatsu, “Oxygen Functionalization of Multiwall Carbon Nanotubes by Microwave-Excited Surface-Wave Plasma Treatment,” *J. Phys. Chem. C*, vol. 113, no. 18, pp. 7659–7665, 2009.
[107] X. Ren, C. Chen, M. Nagatsu, and X. Wang, “Carbon nanotubes as adsorbents in environmental pollution management: a review,” *Chem. Eng. J.*, 2011.
[108] P. Marques, M. Rosa, and H. Pinheiro, “pH effects on the removal of Cu 2+, Cd 2+ and Pb 2+ from aqueous solution by waste brewery biomass,” *Biosyst. Eng.*, 2000.
[109] C. Lu and C. Liu, “Removal of nickel (II) from aqueous solution by carbon nanotubes,” *J. Chem. Technol.*, 2006.
[110] A. Stafiej and K. Pyrzynska, “Adsorption of heavy metal ions with carbon nanotubes,” *Sep. Purif. Technol.*, 2007.
[111] W. Tang, G. Zeng, J. Gong, Y. Liu, and X. Wang, “Simultaneous adsorption of atrazine and Cu (II) from wastewater by magnetic multi-walled carbon nanotube,” *Chem. Eng.*, 2012.
[112] C. Chen and X. Wang, “Adsorption of Ni (II) from aqueous solution using oxidized multiwall carbon nanotubes,” *Ind. Eng. Chem. Res.*, 2006.
[113] S. Yang, J. Li, D. Shao, J. Hu, and X. Wang, “Adsorption of Ni (II) on oxidized multi-walled carbon nanotubes: effect of contact time, pH, foreign ions and PAA,” *J. Hazard. Mater.*, 2009.
[114] H. Takagi, Y. Soneda, H. Hatori, Z. Zhu, and G. Lu, “Effects of nitric acid and heat treatment on hydrogen adsorption of single-walled carbon nanotubes,” *Aust. J.*, 2007.
[115] M. Toebes, J. van Heeswijk, J. Bitter, and A. Van Dillen, “The influence of oxidation on the texture and the number of oxygen-containing surface groups of carbon nanofibers,” *Carbon N. Y.*, 2004.
[116] S. Hsieh, J. Horng, and C. Tsai, “Growth of carbon nanotube on micro-sized Al 2 O 3 particle and its application to adsorption of metal ions,” *J. Mater. Res.*, 2006.
[117] Y. Zhongguo ke xue yuan. Research Center for Eco-Environmental Sciences. *et al.*, *Journal of environmental sciences.*, vol. 16, no. 2. Elsevier Ltd., 2004.
[118] C. Lu, C. Liu, and G. Rao, “Comparisons of sorbent cost for the removal of Ni 2+ from aqueous solution by carbon nanotubes and granular activated carbon,” *J. Hazard. Mater.*, 2008.
[119] Y. Li, Z. Di, J. Ding, D. Wu, Z. Luan, and Y. Zhu, “Adsorption thermodynamic, kinetic and desorption studies of Pb 2+ on carbon nanotubes,” *Water Res.*, 2005.
[120] C. Lu, H. Chiu, and C. Liu, “Removal of zinc (II) from aqueous solution by purified carbon nanotubes: kinetics and equilibrium studies,” *Ind. Eng. Chem. Res.*, 2006.
[121] H. Li, L. Pan, Y. Zhang, and Z. Sun, “Ferric ion adsorption and electrodesorption by carbon nanotubes and nanofibres films,” *Water Sci. Technol.*, 2009.
[122] X. Ren, C. Chen, M. Nagatsu, and X. Wang, “Carbon nanotubes as adsorbents in environmental pollution management: a review,” *Chem. Eng. J.*, 2011.
[123] G. Rao, C. Lu, and F. Su, “Sorption of divalent metal ions from aqueous solution by

carbon nanotubes: a review," *Sep. Purif. Technol.*, 2007.
[124] H. Wang, A. Zhou, F. Peng, H. Yu, and J. Yang, "Mechanism study on adsorption of acidified multiwalled carbon nanotubes to Pb (II)," *J. Colloid Interface*, 2007.
[125] R. Long and R. Yang, "Carbon nanotubes as a superior sorbent for nitrogen oxides," *Ind. Eng. Chem. Res.*, 2001.
[126] J. Liang *et al.*, "Facile synthesis of alumina-decorated multi-walled carbon nanotubes for simultaneous adsorption of cadmium ion and trichloroethylene," *Chem. Eng. J.*, vol. 273, pp. 101–110, 2015.
[127] G. Rao, C. Lu, and F. Su, "Sorption of divalent metal ions from aqueous solution by carbon nanotubes: a review," *Sep. Purif. Technol.*, 2007.
[128] S.-H. Hsieh and J.-J. Horng, "Adsorption behavior of heavy metal ions by carbon nanotubes grown on microsized Al2O3 particles," *J. Univ. Sci. Technol. Beijing, Miner. Metall. Mater.*, vol. 14, no. 1, pp. 77–84, Feb. 2007.
[129] W. Mi, Y. S. Lin, and Y. Li, "Vertically aligned carbon nanotube membranes on macroporous alumina supports," 2007.
[130] B. Lee *et al.*, "A carbon nanotube wall membrane for water treatment," *Nat. Commun.*, vol. 6, p. 7109, May 2015.
[131] M. Ahmadzadeh Tofighy and T. Mohammadi, "Nickel ions removal from water by two different morphologies of induced CNTs in mullite pore channels as adsorptive membrane," *Ceram. Int.*, vol. 41, no. 4, pp. 5464–5472, 2015.
[132] S. Barma and B. Mandal, "Effects of sintering temperature and initial compaction load on alpha-alumina membrane support quality," *Ceram. Int.*, 2014.
[133] W. Qin, C. Peng, M. Lv, and J. Wu, "Preparation and properties of high-purity porous alumina support at low sintering temperature," *Ceram. Int.*, 2014.
[134] K. Shafiei and M. Kazemimoghaddam, "An investigation on manufacturing of alumina microfiltration membranes," *Water Treat.*, 2015.
[135] O. Lyckfeldt and J. Ferreira, "Processing of porous ceramics by 'starch consolidation,'" *J. Eur. Ceram. Soc.*, 1998.
[136] M. Ghaderi, M. Afarani, and G. Roudini, "Synthesis of alumina porous supports via different compaction routes: vibration and pressing," *J. Chem. Tech. Met.*, 2013.
[137] T. Laoui, F. Patel, and N. Saheb, "Manufacture of microporous ceramic layer by suspension–sedimentation for filtration applications," *Proc.*, 2013.
[138] Ihsanullah *et al.*, "Fabrication and antifouling behaviour of a carbon nanotube membrane," *Mater. Des.*, vol. 89, pp. 549–558, 2016.
[139] T. Ostrowski and J. Rödel, "Evolution of mechanical properties of porous alumina during free sintering and hot pressing," *J. Am. Ceram. Soc.*, 1999.
[140] Z. Deng, T. Fukasawa, and M. Ando, "Microstructure and mechanical properties of porous alumina ceramics fabricated by the decomposition of aluminum hydroxide," *J.*, 2001.
[141] D. Green, C. Nader, and R. Brezny, "Elastic behaviour of partially-sintered alumina," *Proc. Symp. Sinter. Adv. Ceram. ...*, 1988.
[142] D. Lam, F. Lange, and A. Evans, "Mechanical properties of partially dense alumina produced from powder compacts," *J. Am.*, 1994.
[143] S. Nanjangud and R. Brezny, "Strength and Young's modulus behavior of a partially sintered porous alumina," *J. Am.*, 1995.
[144] C. Kawai and A. Yamakawa, "Effect of porosity and microstructure on the strength

of Si3N4: designed microstructure for high strength, high thermal shock resistance, and facile machining," *J. Am. Ceram.*, 1997.
[145] G. Li, Z. Jiang, A. Jiang, and L. Zhang, "Strengthening of porous Al2O3 ceramics through nanoparticle addition," *Nanostructured Mater.*, 1997.
[146] D. Chakravarty, H. Ramesh, and T. Rao, "High strength porous alumina by spark plasma sintering," *J. Eur. Ceram.*, 2009.
[147] F. Inam, H. Yan, D. Jayaseelan, and T. Peijs, "Electrically conductive alumina–carbon nanocomposites prepared by spark plasma sintering," *J. Eur.*, 2010.
[148] A. Standard, "Standard test method for water absorption, bulk density, apparent porosity and apparent specific gravity for fired whiteware products, Annual Book," *Annu. B. ASTM Stand.*
[149] D. Cranmer and D. Richerson, *Mechanical testing methodology for ceramic design and reliability*. 1998.
[150] A. Afkhami, M. Saber-Tehrani, and H. Bagheri, "Simultaneous removal of heavy-metal ions in wastewater samples using nano-alumina modified with 2, 4-dinitrophenylhydrazine," *J. Hazard. Mater.*, 2010.
[151] R. M. German, *Sintering theory and practice*. Wiley, 1996.
[152] K. Niihara, "New design concept of structural ceramics," *J. Ceram. Soc. Japan*, 1991.
[153] T. Ostrowski and J. Rödel, "Evolution of mechanical properties of porous alumina during free sintering and hot pressing," *J. Am. Ceram. Soc.*, 1999.
[154] Z. Deng, T. Fukasawa, and M. Ando, "Microstructure and mechanical properties of porous alumina ceramics fabricated by the decomposition of aluminum hydroxide," *J.*, 2001.
[155] C. Falamaki, M. Afarani, and A. Aghaie, "Initial sintering stage pore growth mechanism applied to the manufacture of ceramic membrane supports," *J. Eur. Ceram.*, 2004.
[156] S. Ananthakumar and K. Warrier, "Extrusion characteristics of alumina–aluminium titanate composite using boehmite as a reactive binder," *J. Eur. Ceram. Soc.*, 2001.
[157] R. Spriggs and T. Vasilos, "Effect of grain size on transverse bend strength of alumina and magnesia," *J. Am. Ceram.*, 1963.
[158] D. Cranmer and D. Richerson, *Mechanical testing methodology for ceramic design and reliability*. 1998.
[159] T. Naiya, A. Bhattacharya, and S. Das, "Adsorption of Cd (II) and Pb (II) from aqueous solutions on activated alumina," *J. Colloid Interface*, 2009.
[160] A. Abbas, A. Al-Amer, T. Laoui, and M. Al-Marri, "Heavy metal removal from aqueous solution by advanced carbon nanotubes: critical review of adsorption applications," *Sep.*, 2016.

Vitae

Name: :Hafiz Khurram Shahzad

Nationality: :Pakistan

Date of Birth: :12/25/1988

Email: :mirzakhurram66@gmail.com

Academic Background: **MS in Materials Science and Engineering, May 2017**

King Fahd University of Petroleum and Minerals (KFUPM), Dhahran. KSA

B.Sc. Metallurgy and Materials Engineering, Nov. 2012

Institute of Advanced Materials (IAM), Bahauddin Zakariya University (BZU), Multan. Pakistan

Conference Presentations

1. Tahar Laoui, **H. K. Shahzad**, Ihsanullah, Faheemuddin Patel, Nasser Al-Aqeeli, Muataz Atieh, 'Processing of Activated Carbon (AC)/Carbon Nanotubes-Alumina Composite Membranes for Water Filtration.' 11th International Conference on Ceramic Materials and Components for Energy and Environmental Applications (CMCEE-11), Vancouver, Canada 14-19 June 2015.

2. Tahar Laoui, **H. K. Shahzad**, Mohammed A. Hussein, Faheemuddin Patel, Muataz Atieh, Nasser Al-Aqeeli, "Development and Characterization of Alumina-CNT Porous Membranes", NanoMaterials for Energy and Environment - NanoMatEn 2016 conference, Paris, France, 1-3 June 2016

3. H. K. Shahzad, M.A. Hussein, Faheemuddin Patel, Nasser Al-Aqeeli, Muataz A. Atieh, Tahar Laoui, 'Processing of Alumina-Carbon Nanotubes Composite Membranes for Water Filtration Applications.' The 4th Saudi International Nanotechnology Conference (SINC 2016), Dhahran, Kingdom of Saudi Arabia 25-27 October, 2016